



Minerva Access is the Institutional Repository of The University of Melbourne

Author/s:

Deng, J;Lu, C;Liu, C;Oveissi, S;Fairlie, WD;Lee, EF;Bilsel, P;Puthalakath, H;Chen, W

Title:

Influenza A virus infection-induced macroautophagy facilitates MHC class II-restricted endogenous presentation of an immunodominant viral epitope

Date:

2021-05-01

Citation:

Deng, J., Lu, C., Liu, C., Oveissi, S., Fairlie, W. D., Lee, E. F., Bilsel, P., Puthalakath, H. & Chen, W. (2021). Influenza A virus infection-induced macroautophagy facilitates MHC class II-restricted endogenous presentation of an immunodominant viral epitope. *FEBS Journal*, 288 (10), pp.3164-3185. <https://doi.org/10.1111/febs.15654>.

Persistent Link:

<https://hdl.handle.net/11343/276757>

1

2 DR HAMSA PUTHALAKATH (Orcid ID : 0000-0001-5178-1175)

3 DR WEISAN CHEN (Orcid ID : 0000-0002-5221-9771)

4

5

6 Received Date : 23-Jul-2020

7 Revised Date : 27-Sep-2020

8 Accepted Date : 02-Dec-2020

9 Article type : Original Article

10

11

12 **Color: Fig 1-9**13 **Influenza A virus infection-induced macroautophagy facilitates MHC class II-**  
14 **restricted endogenous presentation of an immunodominant viral epitope**15 Jieru Deng\*, Chunni Lu<sup>\*,†</sup>, Chuanxin Liu\*, Sara Oveissi\*, W. Douglas Fairlie<sup>\*,‡,§</sup>,16 Erinna F. Lee<sup>\*,‡,§</sup>, Pamuk Bilsel<sup>¶</sup>, Hamsa Puthalakath\* and Weisan Chen<sup>\*1,2</sup>

17

18 \*Department of Biochemistry and Genetics, La Trobe Institute for Molecular Science,  
19 La Trobe University, Bundoora, Victoria 3086, Australia

20 †School of Medicine, Deakin University, Waurn Ponds, Victoria 3217, Australia

21 ‡Olivia Newton-John Cancer Research Institute, Heidelberg, Victoria 3084, Australia.

22 §School of Cancer Medicine, La Trobe University, Melbourne, Victoria 3084, Australia.

23 ¶FluGen Inc., Madison, WI 53711, USA

24

25 <sup>1</sup>To whom correspondence should be addressed: [weisan.chen@latrobe.edu.au](mailto:weisan.chen@latrobe.edu.au)

26

This is the author manuscript accepted for publication and has undergone full peer review but has not been through the copyediting, typesetting, pagination and proofreading process, which may lead to differences between this version and the Version of Record. Please cite this article as [doi: 10.1111/FEBS.15654](https://doi.org/10.1111/FEBS.15654)

This article is protected by copyright. All rights reserved

27 <sup>2</sup>This project was supported by the NHMRC program grant 567122 to WC.

28

29 **Running title:** IAV induced-autophagy facilitates endogenous MHC-II presentation

30

31 **Key words:** Influenza A virus, macroautophagy, MHC-II, antigen presentation, CD4<sup>+</sup>  
32 T cell

33 **Abbreviations:** 3-MA, 3-methyladenine; APCs, antigen presenting cells; *ATGs*,  
34 autophagy-related genes; BAL, bronchoalveolar lavage; BFA, brefeldin A; BMDCs,  
35 Bone-Marrow Derived Dendritic cells; CMA, chaperone-mediated autophagy; CLIP,  
36 class II-associated invariant chain peptide; CRISPR, clustered regularly interspaced  
37 short palindromic repeats; EBSS, Earle's Balanced Salt Solution; EBV, Epstein-Barr  
38 virus; ER, endoplasmic reticulum; IAV, influenza A virus; ICS, intracellular cytokine  
39 staining; IIV, inactivated influenza vaccines; LAIV, live-attenuated influenza vaccines;  
40 LC3, light-chain kinase 3; M2SR, M2-deficient single replication vaccine virus; MHC,  
41 major histocompatibility complex; MHC-I, MHC class I molecule; MHC-II, MHC  
42 class II molecule; MIIC, MHC class II compartment

43

44 **Abstract**

45 CD4<sup>+</sup> T cells recognize peptides presented by major histocompatibility complex class  
46 II molecules (MHC-II). These peptides are generally derived from exogenous antigens.  
47 Macroautophagy has been reported to promote endogenous antigen presentation in viral  
48 infections. However, whether influenza A virus (IAV) infection-induced  
49 macroautophagy also leads to endogenous antigen presentation through MHC-II is still  
50 debated. In this study, we show that IAV infection leads to endogenous presentation of  
51 an immunodominant viral epitope NP<sub>311-325</sub> by MHC-II to CD4<sup>+</sup> T cells.  
52 Mechanistically, such MHC-II-restricted endogenous IAV antigen presentation  
53 requires *de novo* protein synthesis as it is inhibited by the protein synthesis inhibitor  
54 cycloheximide, and a functional ER-Golgi network as it is totally blocked by Brefeldin

This article is protected by copyright. All rights reserved

55 A. These results indicate that MHC-II-restricted endogenous IAV antigen presentation  
56 is dependent on *de novo* antigen and/or MHC-II synthesis, and transportation through  
57 the ER-Golgi network. Furthermore, such endogenous IAV antigen presentation by  
58 MHC-II is enhanced by TAP deficiency, indicating some antigenic peptides are of  
59 cytosolic origin. Most importantly, the bulk of such MHC-II-restricted endogenous  
60 IAV antigen presentation is blocked by autophagy inhibitors (3-MA and E64d) and  
61 deletion of autophagy related genes, such as *Beclin1* and *Atg7*. We have further  
62 demonstrated that in dendritic cells, IAV infection prevents autophagosome-lysosome  
63 fusion and promotes autophagosome fusion with MHC Class II compartment (MIIC),  
64 which likely promotes endogenous IAV antigen presentation by MHC-II. Our results  
65 provide strong evidence that IAV infection-induced autophagosome formation  
66 facilitates endogenous IAV antigen presentation by MHC-II to CD4<sup>+</sup> T cells. The  
67 implication for influenza vaccine design is discussed.

68

## 69 **Introduction**

70 CD4<sup>+</sup> T cells not only provide "help" to B cells to improve the humoral immune  
71 response, but also play a significant role in helping the CD8<sup>+</sup> T cell response, especially  
72 during T cell memory formation and recall [1]. In general, CD4<sup>+</sup> T cells recognize  
73 antigenic peptides presented by major histocompatibility complex class II molecules  
74 (MHC-II) on professional antigen presenting cells (APCs), including B cells,  
75 macrophages and dendritic cells (DCs). MHC-II generally present peptides derived  
76 from "exogenous" antigen engulfed by APCs, as they cannot normally pick up  
77 endogenous peptides in the endoplasmic reticulum (ER) because their peptide-binding  
78 clefts are occupied by the chaperone invariant chain [2]. Whereas CD8<sup>+</sup> T cell  
79 activation depends on the recognition of pMHC-I expressed on most cell types. MHC-  
80 I pick up "endogenous" peptides in the ER as they are largely derived from antigens  
81 synthesized inside the APC, degraded by the proteasomes and transported into the ER  
82 by transporters associated with antigen processing (TAP) [3]. However, there are

83 exceptions. For example, exogenous antigens can be presented by MHC-I through a  
84 well-established process known as "cross-presentation" [4, 5]. Similarly, endogenous  
85 antigens such as some self-antigens [6], tumor antigens [7-9], and viral antigens [10-  
86 12] can be presented by MHC-II to CD4<sup>+</sup> T cells. The endogenous IAV antigen  
87 presentation to CD4<sup>+</sup> T cells was first reported by Gueguen and colleagues [13], and  
88 later by Schmid *et al.* [14], and more recently, our lab showed that human CD4<sup>+</sup> T cells  
89 could recognize IAV-infected, EBV-transformed B cell lines [15]. However, the  
90 mechanism associated with endogenous IAV antigen presentation by MHC-II has been  
91 poorly established. Recently, some endogenous antigen presentation was reported to be  
92 related to macroautophagy activity [16-18]. EBNA1, a nuclear antigen from Epstein-  
93 Barr virus (EBV), was the first reported pathogenic antigen recognized by CD4<sup>+</sup> T cells  
94 through macroautophagy-involved endogenous antigen presentation [19]. Furthermore,  
95 virus infection-induced macroautophagy has been shown to activate HIV-specific CD4<sup>+</sup>  
96 T cells [20]. These findings suggest that macroautophagy activity could enhance  
97 endogenous antigen processing and presentation through the MHC-II-restricted  
98 pathway. As both EBV and HIV cause chronic infection, it is not clear whether acute  
99 virus infection, such as IAV infection, could also cause such endogenous antigen  
100 presentation by MHC-II.

101 Influenza virus infection causes half a million deaths annually worldwide [21].  
102 Inactivated influenza vaccines (IIVs) are commonly used for protecting against  
103 influenza virus infection. However, their efficacy needs to be improved [22-24]. There  
104 are three potential reasons for the lower than expected efficacy of IIVs. First, as IIVs  
105 aim at inducing a humoral immune response towards the influenza virus surface  
106 proteins Hemagglutinin (HA) and Neuraminidase (NA) [25], the frequent mutations in  
107 HA and NA often render such vaccinated antibodies ineffective [26]. Second, IIVs  
108 induce limited CD8<sup>+</sup> T cell-responses [27, 28], as they do not carry sufficient internal  
109 antigens on one hand, whilst on the other hand the minimal internal antigens they do  
110 carry have to follow the less efficient cross-presentation pathway [29, 30]. Furthermore,

111 it is possible that CD4<sup>+</sup> T cell priming during IAV infection might rely on endogenous  
112 antigen presentation by MHC-II and the presented epitopes might be different from  
113 those derived from exogenous antigens. Therefore, understanding the nature of IAV  
114 antigen presentation to CD4<sup>+</sup> T cells during IAV infection could potentially provide  
115 insights into anti-IAV cellular and humoral immune responses for future novel  
116 influenza vaccine design.

117 Macroautophagy is a bulk degradation pathway by which intracellular constituents are  
118 cleared and recycled in the cytosol for the maintenance of cellular homeostasis [31, 32].  
119 During this process, more than 36 autophagy-related genes (*ATGs*) are involved in  
120 regulating autophagosome formation and autophagic flux [31, 33]. Previous studies  
121 have shown that IAV infection induces autophagosome formation [34, 35]. Moreover,  
122 it was reported that the M2 protein played a critical role in blocking the fusion of  
123 autophagosomes with lysosomes [36, 37]. Furthermore, an IAV antigen M1 covalently  
124 linked to a key autophagy molecule LC3 led to M1 endogenous antigen presentation by  
125 MHC-II to CD4<sup>+</sup> T cells [14]. In contrast, more recently published data demonstrated  
126 endogenous IAV antigen presentation by MHC-II without the involvement of  
127 macroautophagy in this process [11, 38]. Thus, the role of macroautophagy during  
128 endogenous IAV antigen presentation through MHC-II-mediated pathway is still  
129 debated. Further characterizing IAV-infection-induced macroautophagy in APCs and  
130 its potential role (or the lack of it) in endogenous antigen presentation is of vital  
131 importance for better understanding the anti-IAV T helper response.

132 In this study, we have shown that IAV infection in DCs induces autophagosome  
133 formation, prevents autophagosome-lysosome fusion and promotes autophagosome  
134 fusion with MHC class II compartment (MIIC). As a result, we demonstrate for the first  
135 time that IAV infection-induced autophagosome accumulation contributes to  
136 endogenous IAV antigen presentation by MHC-II.

137

## 138 **Results**

139 **IAV infection leads to endogenous IAV antigen presentation by MHC-II *in vitro***  
140 We previously reported that IAV infection leads to endogenous IAV antigen  
141 presentation by MHC-II to CD4<sup>+</sup> T cells in EBV transformed human B cells [15]. To  
142 explore the associated molecular mechanisms, we utilized the H-2<sup>b</sup>-restricted IAV-  
143 specific CD4<sup>+</sup> T cell epitopes identified previously [39] (Table 1). We first intranasally  
144 infected B6 mice with 100 pfu of PR8. 10 days post infection (dpi), T cells recovered  
145 in the bronchoalveolar lavage (BAL) and the spleen were assessed by an *ex vivo*  
146 intracellular cytokine staining (ICS) assay with the 17 reported MHC-II-restricted  
147 peptides, including NP epitopes (NP<sub>260-273</sub>, NP<sub>276-290</sub>, and NP<sub>311-325</sub>), PB2 epitopes  
148 (PB2<sub>91-105</sub> and PB2<sub>106-120</sub>) and PA epitopes (PA<sub>316-330</sub> and PA<sub>456-470</sub>). We confirmed the  
149 CD4<sup>+</sup> T cell immunodominance hierarchy specific to the IAV peptides, among which  
150 NP<sub>311-325</sub>-specific T cells were the most immunodominant both in the BAL and spleen  
151 cell populations (Figure 1A). Subsequently, we generated immunodominant NP<sub>311-325</sub>-  
152 specific CD4<sup>+</sup> and NP<sub>366-374</sub>-specific CD8<sup>+</sup> T cell lines [40], both with high purity and  
153 are highly sensitive to their cognate antigenic peptides as shown in Figure 1B. Using  
154 these T cell lines, we were able to demonstrate that PR8-infected BMDCs *in vitro* were  
155 able to present endogenous IAV antigens onto both MHC-I- and MHC-II-restricted  
156 pathways (Figure 1C). Meanwhile, CD4<sup>+</sup> T cell activation was abolished when BMDCs  
157 were infected with heat-inactivated PR8, although preheated NP protein was still  
158 presented to NP<sub>311-325</sub>-specific CD4<sup>+</sup> T cells *via* the exogenous antigen processing and  
159 presentation pathway (Figure 1D). Additionally, we found that endogenous IAV  
160 antigen presentation by MHC-II was almost completely blocked by a protein synthesis  
161 inhibitor cycloheximide (CHX) [41] (Figure 1E) and totally blocked by an ER to Golgi  
162 transition inhibitor Brefeldin A (BFA) (Figure 1F). These results further confirm that  
163 NP<sub>311-325</sub> presentation after IAV infection relies on IAV infection and replication. The  
164 BFA blockade result likely indicates that the endogenous antigen presentation to CD4<sup>+</sup>  
165 T cells requires *de novo* synthesized MHC-II. In contrast, the subdominant, PB2<sub>106-120</sub>-  
166 specific CD4<sup>+</sup> T cells could not respond endogenous IAV antigen presentation *in vitro*

167 (Figure 2), indicating that the efficiency of endogenous IAV antigen presentation to  
168 CD4<sup>+</sup> T cells *in vitro* is epitope dependent.

169

### 170 **Endogenous IAV antigen processing and presentation by MHC-II is reduced by** 171 **TAP *in vitro***

172 MHC-I binding peptides are usually generated in the cytosol by proteasomes and  
173 delivered into the ER through the TAP1 and TAP2 heterodimer [42]. In contrast, MHC-  
174 II presents exogenous antigens *via* a TAP-independent route. However, whether the  
175 MHC-II-mediated endogenous IAV antigen presentation required functional TAP was  
176 not known. To address this, *Tap1*-deficient BMDCs and mice were infected with IAV  
177 and the CD8<sup>+</sup> and CD4<sup>+</sup> T cell activation was then determined. We found that MHC-I-  
178 restricted endogenous IAV antigen presentation was totally blocked in IAV-infected  
179 *Tap1*<sup>-/-</sup> BMDCs as expected (Figure 3A, left), and similar results were obtained from *in*  
180 *vivo* experiments (Figure 3B, left). Interestingly, the endogenous IAV antigen  
181 presentation of NP<sub>311-325</sub> to its specific CD4<sup>+</sup> T cells was enhanced in *Tap1*<sup>-/-</sup> BMDCs *in*  
182 *vitro* (Figure 3A, right), although such an enhanced CD4<sup>+</sup> T cell response was not  
183 observed *ex vivo* (Figure 3B, right). Similarly, we verified that B6.*Tap1*<sup>-/-</sup> mice lacked  
184 the CD8<sup>+</sup> T cell population in their spleens, indicating their *Tap1* knockout status  
185 (Figure 3C) [43]. These results suggest that MHC-II-restricted endogenous IAV antigen  
186 processing and presentation is impaired by the presence of functional TAP.

187

### 188 **IAV infection induce autophagosome accumulation in dendritic cells**

189 IAV infection induces macroautophagy which enhances IAV replication [35]. To  
190 further elucidate the mechanisms of endogenous IAV antigen presentation, we  
191 investigated the potential involvement of autophagy pathway. The conversion of the  
192 soluble microtubule-associated protein 1 light chain kinase 3 (LC3-I) to lipidated LC3-  
193 II, which is subsequently associated with the autophagic membrane, is considered as  
194 the most important marker for autophagosome formation [44]. Besides, *Atg6/Beclin1*

195 activates phosphatidylinositol 3-phosphate (PI3P) deposition at membrane sites to  
196 facilitate autophagosome formation and *Atg7* contributes to autophagosome formation  
197 *via* its involvement in LC3 conversion [45]. Furthermore, the degradation of  
198 SQSTM1/p62 is commonly used as a marker for autophagic flux - reflecting  
199 autophagosome:lysosome fusion and the subsequent clearance of intracellular  
200 constituents [46]. To determine whether IAV infection regulates macroautophagy in  
201 APCs, these autophagy-related protein expression levels were assessed by Western  
202 blotting and confocal microscopy in IAV-infected BMDCs and DC2.4 cells, a DC-like  
203 cell line [47]. Our results showed that LC3 conversion increased in both PR8- and X31-  
204 infected BMDCs relative to that in mock-infected BMDCs (Figure 4A). In addition, the  
205 PR8- and X31-infected BMDCs showed increased expression levels of Beclin1 and  
206 *Atg7* compared to non-infected group. More importantly, the autophagosome marker  
207 protein LC3-II increased in a time-dependent fashion in the infected BMDCs (Figure  
208 4A). Similar results were obtained from PR8- and X31-infected DC2.4 cells (Figure  
209 4B). However, here we could not detect p62 degradation within 24 h of virus infection,  
210 although IAV matrix protein M1 accumulated during this time (Figures 4A and 4B).  
211 Moreover, the increased *Atg7* and Beclin1 expression, and the lipidated LC3-II in PR8-  
212 or X31-infected DC2.4 cells were also confirmed by confocal microscopy (Figure 4C).  
213 Taken together, we demonstrate that IAV infection increases *Atg7* and Beclin1  
214 expression and LC3 conversion in DCs, although there is no evidence of  
215 autophagosome fusion with lysosome as indicated by lack of p62 degradation.  
216 To further confirm whether the IAV infection-induced macroautophagy leads to  
217 increased autophagic flux, we transduced DC2.4 cells with a tandem mCherry-EGFP-  
218 LC3B reporter utilizing a retroviral vector [48]. This reporter system detects autophagic  
219 flux based on the fact that GFP is unstable in acidic pH, while mCherry is not. Therefore,  
220 the green fluorescence will be decreased after autophagosomes fuse with lysosomes.  
221 Earle's Balanced Salt Solution (EBSS) was used as a positive control as it induces  
222 functional macroautophagy in cells through starvation [49, 50]. Western blotting

223 showed increased p62 degradation and LC3 conversion in EBSS-treated DC2.4 cells,  
224 compared to untreated control (Figure 4D).

225 Having established the system, we next examined PR8- or X31-infected, mock-infected  
226 or EBSS treated DC2.4-mCherry-EGFP-LC3B cells by flow cytometry. Importantly,  
227 reduced GFP fluorescence was only observed in the EBSS treated group (Figure 4E),  
228 indicating the autophagosomes did not fuse with lysosomes during IAV infection.  
229 Collectively, IAV infection induces autophagosome formation in the absence of  
230 autophagic flux in DCs.

231

### 232 **M2 protein is not required for blocking the fusion of autophagosomes with** 233 **lysosomes after IAV infection**

234 Previous studies reported that the IAV M2 protein played a critical role in blocking  
235 autophagosome-lysosome fusion [36, 37]. To determine whether this is the mechanism  
236 in our study, an M2-deficient single-cycle replication virus (M2SR) on the PR8  
237 backbone was utilized [51]. Unexpectedly, we did not observe p62 degradation in both  
238 PR8-infected DC2.4 cells and M2SR-infected DC2.4 cells assessed by Western blotting  
239 at different time points after virus infection. Virus M1 proteins were detected in both  
240 PR8 and M2SR infected cells confirming infected cell status, while virus M2 proteins  
241 only accumulated in PR8-infected cells, but not in M2SR-infected cells, confirming M2  
242 knockout status (Figure 4F). Furthermore, the mCherry-GFP reporter system did not  
243 show any difference between the PR8 and M2SR infected cells, and the GFP  
244 fluorescence downregulation was again only detected in the EBSS-treated control  
245 group (Figure 4G). Taken together, in our system, M2 does not contribute to blocking  
246 fusion of the autophagosome with the lysosome during IAV-infection-induced  
247 macroautophagy.

248

### 249 **Inhibition of autophagy impairs endogenous IAV antigen presentation by MHC-**

250 **II**

251 To verify the role of IAV infection-induced autophagosome accumulation during  
252 MHC-II restricted endogenous IAV antigen processing and presentation, autophagy  
253 inhibitors 3-methyladenine (3-MA) and E64d were used to downregulate autophagy  
254 activity. BMDCs or DC2.4 cells were IAV-infected in the presence of 3-MA or E64d  
255 for 24 h and autophagy-related proteins were assessed by Western blotting. LC3  
256 conversion was decreased in IAV-infected BMDCs after 3-MA (at 5 mM) treatment,  
257 and no significant LC3-II turnover was observed in IAV-infected BMDCs with E64d  
258 (10 µg/ml) treatment, which again reflected IAV infection induced autophagy but in the  
259 absence of autophagic flux (Figure 5A). Importantly, drug treatment did not  
260 significantly affect cell viability as assessed by the AlamarBlue assay (Figure 5B). To  
261 determine whether antigen processing and presentation was altered, 3-MA or E64d  
262 treated IAV-infected BMDCs were used as APCs to stimulate NP<sub>311-325</sub>-specific CD4<sup>+</sup>  
263 T cells. Both 3-MA or E64d treatment clearly diminished CD4<sup>+</sup> T cell activation  
264 (Figure 5C), although these inhibitors did not significantly inhibit IAV infection judged  
265 by NP staining and the mean fluorescence intensity (MFI) in NP<sup>+</sup> BMDCs (Figure 5D).  
266 Similar results were obtained from autophagy inhibitor-treated IAV-infected DC2.4  
267 cells (Figures 5E and 5F). These data indicate endogenous IAV antigen presentation by  
268 MHC-II is at least partially autophagy dependent.

269

### 270 **Knocking out autophagy-related genes *Beclin1* and *Atg7* decreases endogenous** 271 **IAV antigen presentation by MHC-II**

272 To further explore whether the IAV-infection-induced autophagosome accumulation  
273 contributed to endogenous IAV antigen presentation to CD4<sup>+</sup> T cells, we turned to a  
274 *Cre-loxP* based conditional *Beclin1* knockout mouse model (B6.BecConRosa) under  
275 the control of estrogen receptor [52-54]. Tamoxifen was given to B6.BecConRosa mice  
276 and control B6 mice for 5 days in order to specifically delete the *Beclin1* gene in these  
277 mice, resulting in nearly complete deletion of *Beclin1* expression in various tissues  
278 examined, including BMDCs (Figure 6A). The lack of *Beclin1* expression resulted in

279 slightly decreased IAV infection efficiency as slightly fewer Bec BMDCs expressed  
280 NP than those among B6 BMDCs. However, the MFI of NP<sup>+</sup> BMDCs were on a similar  
281 level between B6 BMDCs and Bec BMDCs (Figure 6B). Importantly, endogenous IAV  
282 antigen presentation was significantly decreased to less than 1/3 of that detected in B6  
283 BMDCs (Figure 6C), indicating Beclin1 expression was essential for endogenous IAV  
284 antigen presentation by MHC-II.

285 As *Beclin1* is involved not only in autophagy but also other biological processes, such  
286 as apoptosis and endocytic trafficking [55-57], to more specifically address if  
287 autophagy is a key contributing factor, we turned to a lentiviral-based CRISPR/Cas9  
288 system and created *Beclin1* and *Atg7* single knockout DC2.4 cell lines. Gene knockout  
289 was confirmed by Western blotting and Sanger sequencing (Figure 7A, 7B and 7C).  
290 Interestingly, DC2.4-*Beclin1*<sup>-/-</sup> cells, but not DC2.4-*Atg7*<sup>-/-</sup> cells, showed slightly  
291 reduced percentage of NP<sup>+</sup> cells after infection with IAV PR8 strain when compared to  
292 control DC2.4-*FgH1tUTG* cells (cells transduced with empty vector) and the MFI of  
293 NP<sup>+</sup> DC2.4 cells among these cells were at the same level (Figure 7D). Importantly,  
294 both DC2.4-*Beclin1*<sup>-/-</sup> and DC2.4-*Atg7*<sup>-/-</sup> cells showed significantly reduced, but almost  
295 identical, endogenous IAV antigen presentation to NP<sub>311-325</sub>-specific CD4<sup>+</sup> T cells  
296 compared to again the IAV-infected DC2.4-*FgH1tUTG* control cells (Figure 7E). As  
297 *Atg7*'s main role is in autophagy [58], these results further strengthen our previous  
298 observation made using the conditional *Beclin1* knockout BMDCs.

299 Comber *et al.* showed clearly that IAV infection induced macroautophagy activity in  
300 APCs. However, they did not observe decreased endogenous IAV antigen presentation  
301 using *Atg7*-siRNA or *Atg5*-siRNA knockdown BMDCs and *ex vivo* T cell readout in an  
302 ELISpot assay [38]. They therefore argued that macroautophagy did not play a  
303 significant role in promoting endogenous IAV antigen presentation by MHC-II. As our  
304 above experiments were all performed with a single epitope specific CD4<sup>+</sup> T cell line,  
305 we were concerned that the endogenous IAV antigen presentation might be  
306 significantly biased by such an *in vitro* T cell line in our study. We therefore performed

307 the assays described above, this time using *ex vivo* polyclonal T cells derived from PR8  
308 intranasally infected B6 mice. Clearly, both DC2.4-*Beclin1*<sup>-/-</sup> and DC2.4-*Atg7*<sup>-/-</sup> cells  
309 showed significantly decreased endogenous IAV antigen presentation to primary CD4<sup>+</sup>  
310 T cells derived from both BAL washes and spleens compared to the DC2.4-*FgH1tUTG*  
311 control cells (Figure 8A).

312 Miller *et al.* identified 17 CD4<sup>+</sup> T cell epitopes in B6 mice through an overlapping  
313 peptide screen [11]. Thirteen of these peptides, ranging from 15AA to 17AA and  
314 including seven previously unreported ones (NP<sub>45-61</sub>, NP<sub>47-63</sub>, NP<sub>52-68</sub>, HA<sub>16-32</sub>, NS1<sub>19-35</sub>,  
315 NA<sub>25-39</sub>, NA<sub>41-55</sub>, NA<sub>110-124</sub>, PA<sub>15-31</sub>, PA<sub>78-93</sub>, PB1<sub>119-135</sub>, PB2<sub>18-34</sub> and PB2<sub>94-110</sub>), were  
316 used to assess endogenous IAV antigen presentation *ex vivo*, and they also concluded  
317 that macroautophagy activity did not contribute to endogenous IAV antigen  
318 presentation [11]. To see whether the different results obtained in theirs and our  
319 experiments were the consequence of using different peptides and assay methods, we  
320 used 18-mers peptides HA<sub>13-30</sub> and HA<sub>19-36</sub> to cover their HA<sub>16-32</sub>; NA<sub>37-54</sub> and NA<sub>43-60</sub>  
321 to cover NA<sub>41-55</sub>; NP<sub>43-60</sub>, NP<sub>49-66</sub> and NP<sub>55-72</sub> to cover NP<sub>45-61</sub>, NP<sub>47-63</sub> and NP<sub>52-68</sub>; and  
322 our NA<sub>25-42</sub> contains their NA<sub>25-39</sub>. These peptides stimulated the biggest T cell  
323 responses in their experiments. We then assessed CD4<sup>+</sup> T cells specific to these 18-mer  
324 peptides along with our peptide penal and the immunodominant NP<sub>311-325</sub> peptide in an  
325 *ex vivo* ICS assay. Unexpectedly, the percentages of activated primary CD4<sup>+</sup> T cells  
326 specific to these reported epitopes were very low both in the BAL wash and the spleen  
327 populations compared to those specific to NP<sub>311-325</sub>, PB2<sub>106-120</sub>, and PA<sub>456-470</sub> (Figure 8B).

328 Taken together, our data acquired from conditional *Beclin1* knockout BMDCs and  
329 independently created *Beclin1* and *Atg7* knockout DC2.4 cell lines all demonstrate that  
330 the bulk of endogenous IAV antigen presentation by MHC-II is regulated by IAV-  
331 induced macroautophagy, which is true for the most immunodominant epitope NP<sub>311-325</sub>  
332 and is also true for the polyclonal CD4<sup>+</sup> T cells.

333

334 **Autophagosomes fuse with MIIC leading to endogenous IAV antigen presentation**  
335 **by MHC-II**

336 To further understand how IAV-infection-induced autophagosome accumulation  
337 promoted endogenous IAV antigen presentation by MHC-II, we investigated the  
338 relationship among IAV nuclear protein (NP), MHC-II, autophagosome and MIIC in  
339 IAV-infected DC2.4 cells through confocal microscopy. First, we detected significant  
340 fluorescent signals corresponding to LC3 puncta and NP in both PR8- and X31-infected  
341 DC2.4 cells at 24 hpi (Figure 9A and 9B). In contrast, the LC3 puncta accumulation  
342 was not observed in mock-infected cells (Figure 9C). A previous study demonstrated  
343 that the fusion of the autophagosome with MIIC in a human epithelial cell line and a  
344 dendritic cell line contributed to CD4<sup>+</sup> T cell activation in an artificial system in which  
345 IAV-M1 was fused with LC3 [14]. In order to determine whether fusion of  
346 autophagosomes with MIIC contributes to endogenous IAV antigen presentation by  
347 MHC-II after IAV infection, the PR8 or X31 infected DC2.4 cells were labelled by  
348 antibodies specific to LC3 and H2-M (a MIIC resident protein responsible for replacing  
349 the CLIP peptide with an antigenic peptide in murine APCs). Fluorescent puncta  
350 corresponding to LC3-II showed co-localization with H2-M (Figure 9A and 9B), which  
351 was not observed in mock-infected cells (Figure 9C). Next, the localization of NP and  
352 MHC-II was analyzed utilizing antibodies specific to NP or I-A<sup>b</sup>, respectively. The  
353 fluorescence puncta of NP were co-localized with the fluorescence puncta of MHC-II  
354 I-A<sup>b</sup> in IAV-infected DC2.4 cells (Figure 9A and 9B). These results indicate that MIIC  
355 obtains IAV antigens from autophagosomes, leading to endogenous IAV antigen  
356 presentation.

357

358 **Discussion**

359 We previously demonstrated endogenous IAV antigen presentation to human CD4<sup>+</sup> T  
360 cells by IAV-infected EBV-transformed B cell lines, although the mechanism was not  
361 further explored [15]. This phenomenon is now confirmed in murine DCs in this study

362 as NP<sub>311-325</sub>-specific CD4<sup>+</sup> T cells recognized IAV-infected BMDCs *in vitro*. Such a  
363 conclusion was supported by several lines of evidence. First, NP<sub>311-325</sub>-specific CD4<sup>+</sup> T  
364 cells only recognized DCs infected by live IAV, but not heat-inactivated IAV. Second,  
365 antigen presentation was completely blocked by BFA in IAV-infected DCs, indicating  
366 the lack of exogenous antigen presentation by surface MHC-II. Finally, CD4<sup>+</sup> T cell  
367 activation by IAV-infected BMDCs was almost completely blocked by protein  
368 synthesis inhibitor CHX.

369 In MHC-I-restricted endogenous and exogenous antigen cross-presentation, TAP plays  
370 a critical role [59]. In our study, the B6.*Tap*<sup>-/-</sup> mice were utilized to see whether  
371 endogenous IAV antigen presentation by MHC-II was also influenced by TAP function.  
372 Interestingly, the endogenous IAV antigen presentation by MHC-II was actually  
373 enhanced in *Tap*<sup>-/-</sup> BMDCs *in vitro*. However, the enhanced CD4<sup>+</sup> T cell response was  
374 not observed in IAV-infected B6.*Tap*<sup>-/-</sup> mice. It is possible that TAP also reduced  
375 endogenous IAV antigen presentation by MHC-II *in vivo*, however, as the endogenous  
376 IAV antigen presentation might be anyway above the level required for T cell priming,  
377 the CD4<sup>+</sup> T cell response in the *Tap*<sup>-/-</sup> mice remained unchanged. We do not believe  
378 that in our system the MHC-II presented peptides are transported by TAP into ER as  
379 MHC-II in the ER are blocked by the invariant chain [60]. Instead, we believe that some  
380 of the cytosolic antigenic peptides transported into the ER by the TAP molecules  
381 become unavailable for endogenous IAV antigen presentation by MHC-II. When TAP  
382 function is absent, such peptides become available to the MHC-II endogenous  
383 presentation pathway and thus the endogenous IAV antigen presentation is enhanced in  
384 *Tap*<sup>-/-</sup> APCs. Therefore, the functional TAP is not required for MHC-II-restricted  
385 endogenous IAV antigen processing.

386 Autophagy is essential for maintaining cellular homeostasis and plays an essential role  
387 in both innate and adaptive immune responses. Our results clearly demonstrated that  
388 IAV infection not only induced autophagosome accumulation in DCs as reflected by  
389 higher Atg7 and Beclin1 expression and increased LC3 conversion in infected cells, but

390 also decreased autophagosome-lysosome fusion reflected by lack of p62 degradation  
391 and GFP quenching in the GFP-mCherry reporter system in IAV-infected cells.  
392 Furthermore, since the M2SR infected cells also showed a lack of p62 degradation and  
393 GFP quenching, we excluded M2 as being the critical factor blocking autophagosome-  
394 lysosome fusion after IAV infection. These data contradict previous reports on M2  
395 blocking autophagosome fusion with lysosome after IAV infection [36, 37]. However,  
396 in either report, no direct evidence was provided to demonstrate the role of M2 in  
397 autophagosome-lysosome fusion, for example, in the absence of M2 during IAV  
398 infection. Our highly sensitive GFP-mCherry tandem reporter system, coupled with an  
399 M2-deficient IAV infection provided direct evidence excluding a role of M2 in  
400 autophagosome-lysosome fusion.

401 Recent studies have shown that the autophagic pathways are involved in endogenous  
402 antigen presentation through MHC-II-restricted pathway [20, 61]. Our results from this  
403 study clearly showed that the MHC-II-restricted endogenous IAV antigen presentation  
404 was significantly inhibited by autophagy inhibitors, or by eliminating autophagy-  
405 related genes *Beclin1* and *Atg7* *in vitro*. 3-MA and E64d treatment inhibit  
406 autophagosome formation [62-64] or inactivate lysosome enzymes respectively [65,  
407 66]. As we were unable to detect autophagosome and lysosome fusion in IAV-infected  
408 DCs, yet NP<sub>311-325</sub> presentation was still significantly diminished by E64d-treated APCs  
409 indicating E64d might inhibit some other step of IAV-induced macroautophagy. This  
410 observation warrants further investigation. Importantly, the results from autophagy  
411 inhibitor-treated APCs were confirmed and strengthened by our results using IAV-  
412 infected *Beclin1*- or *Atg7*-deficient DCs.

413 Intriguingly, macroautophagy has been reported to not contribute to MHC-II- restricted  
414 endogenous antigen presentation during IAV infection [38]. This study showed that  
415 IAV infection induced functional autophagy in fibroblasts and BMDCs reflected by  
416 both autophagosome formation and autophagosome-lysosome fusion. However, no p62  
417 degradation data were provided to support autophagic flux induced by IAV infection.

418 Furthermore, *Atg7* knockdown by siRNA in these cells did not affect endogenous IAV  
419 antigen presentation by MHC-II to *ex vivo* polyclonal CD4<sup>+</sup> T cells derived from PR8-  
420 infected mice. In contrast, our *Beclin1* and *Atg7* knockout APCs showed significant  
421 downregulation on endogenous IAV antigen presentation to similar *ex vivo* polyclonal  
422 CD4<sup>+</sup> T cells. We believe that this discrepancy might be a result of gene knockdown in  
423 their system, compared with total gene knockout used in our study. Hence, it is possible  
424 that the residual *Atg7* expression might be sufficient to support endogenous IAV  
425 antigen presentation by MHC-II to polyclonal CD4<sup>+</sup> T cells. Additionally, Miller *et al.*  
426 extended such an observation using *ex vivo* CD4<sup>+</sup> T cells in an ELISpot assay [11]. As  
427 most CD4<sup>+</sup> T cell epitopes are about 12AA in length, we used 18-mer peptides covering  
428 or containing six of their peptides in an *ex vivo* ICS assay, which is similar to the  
429 ELISpot assay and was shown to yield comparable results [67]. None of the selected  
430 peptides stimulated major CD4<sup>+</sup> T cell response (Figure 8B). It is therefore possible  
431 that macroautophagy-induced changes to endogenous IAV antigen presentation might  
432 have not been properly assessed using such subdominant CD4<sup>+</sup> T cell populations as  
433 they are likely relatively insensitive due to limited overall signals. However, as we used  
434 a high purity T cell line specific to the most dominant IAV CD4<sup>+</sup> T cell epitope NP<sub>311-</sub>  
435 <sub>325</sub>, our assessment is likely more sensitive to such change. Taken together, our results  
436 clearly demonstrate an essential role of autophagy in endogenous IAV antigen  
437 presentation by MHC-II *in vitro*. This conclusion is not only supported by single  
438 epitope-specific T cell line but also by *ex vivo* polyclonal T cells directly derived from  
439 IAV-infected mice.

440 Furthermore, we visualized autophagosomes and MIIC colocalization, indicating  
441 fusion of these two compartments, in IAV-infected DC2.4 cells by confocal microscopy.  
442 These results collectively demonstrate that IAV-specific CD4<sup>+</sup> T cell responses are  
443 regulated significantly by the autophagic pathway-mediated endogenous IAV antigen  
444 presentation. Our study for the first time demonstrates that IAV infection prevents the  
445 autophagosome from fusing with the lysosome, and as a result, the autophagosome

446 delivers cytosolic IAV antigens (including TAP-transportable peptides) into MIIC for  
447 MHC-II presentation to CD4<sup>+</sup> T cells.

448 Our findings could potentially reshape our thinking on endogenous IAV antigen  
449 presentation and, more importantly, future influenza vaccines. Most of the current  
450 licensed influenza vaccines are IIVs. As they do not carry infectious IAV and are  
451 composed largely soluble IAV proteins, they stimulate limited CD4<sup>+</sup> T cell response  
452 through largely exogenous antigen presentation. Our data, and those from others [11,  
453 38] demonstrate the importance of endogenous IAV antigen presentation by MHC-II.  
454 It might be the case that the current IIVs could not provide sufficient CD4<sup>+</sup> T cell  
455 stimulation as they largely do not access endogenous IAV antigen presentation [11, 39].  
456 If some IAV-specific CD4<sup>+</sup> T cells, especially immunodominant CD4<sup>+</sup> T cells, are  
457 primed more efficiently by endogenous IAV antigen presentation under physiological  
458 conditions, and if such epitopes are not efficiently presented *via* the exogenous antigen  
459 presentation provided by the IIVs, it is then possible that the vaccines might not provide  
460 sufficient CD4<sup>+</sup> T cell stimulation. This will obviously affect the magnitude of both  
461 CD8<sup>+</sup> T cell and B cell antibody responses, as CD4<sup>+</sup> T cell responses are required to  
462 assist both CD8<sup>+</sup> T cell memory formation and B cell antibody affinity maturation and  
463 class switching [68, 69]. We believe that a lack of these considerations might partly  
464 explain the lower than expected protective efficacy of current IIVs against influenza  
465 virus infection, especially against IAV infection, in recent years [23, 24]. Hence, the  
466 more effective live-attenuated influenza vaccines (LAIIV) should be taken into  
467 consideration for controlling influenza virus infection. Based on our study, LAIVs  
468 should not only prime specific CD8<sup>+</sup> T cell-mediated immune responses [70], but also  
469 prime sufficient CD4<sup>+</sup> T cell response for supporting B cell-mediated high affinity,  
470 class-switched antibody production. Since live vaccines may have some biosafety  
471 concerns [71, 72], milder live-attenuated IAV viruses, such as the M2SR, would be a  
472 better choice for designing future novel LAIVs. In our study, M2SR infection was  
473 verified to induce autophagosome accumulation in infected DCs similar to that in the

474 PR8 infected DCs. in addition, novel M2SR live vaccines were reported to protect mice  
475 and ferrets against influenza virus [51, 73]. Therefore, M2SR or a similarly altered  
476 influenza virus might have potential as a novel LAIVs' design for the control of human  
477 influenza infections.

478 In summary, endogenous IAV antigens (synthesized within a cell) can be presented  
479 through both MHC-I- and MHC-II-restricted pathways. In the MHC-I-restricted  
480 pathway, endogenous IAV antigens followed the classical endogenous antigen  
481 processing and presentation pathway. In the MHC-II-restricted pathway, endogenous  
482 IAV antigens followed a pathway, which is autophagy-enhanced, influenced by TAP  
483 function and likely relies on newly synthesized viral proteins and MHC-II molecules.

484

## 485 **Materials and methods**

### 486 **Antibodies and reagents**

487 Antibodies for flow cytometry including rat-anti-mouse CD4 (APC and PE-Cy7, clone  
488 GK1.5), rat-anti-mouse CD8 $\alpha$  (eV450, clone 53-6.7) and rat-anti-mouse IFN- $\gamma$  (PE,  
489 clone XMG1.2) were purchased from eBioscience (Waltham, MA USA). Antibodies  
490 for western blotting and confocal microscopy were purchased from various companies:  
491 primary polyclonal rabbit-anti-Atg7, polyclonal rabbit-anti-p62 and polyclonal rabbit-  
492 anti-LC3B (Sigma-Aldrich); rabbit-anti-Beclin1 (clone D40C5) and rabbit-anti-  
493 GPAPDH (clone 14C10) (Cell signalling); anti-mouse MHC-II (I-A/I-E) (clone  
494 M5/114.15.2) and anti-mouse H2-M (clone 2E5A) (BD Biosciences). Anti-NP (clone  
495 HB-65) [74], anti-M1 (clone M2-1C6) [75], and anti-M2 (clone O19) [76] were kind  
496 gifts provided by Dr Jonathan Yewdell, NIAID, NIH (Bethesda, MD, USA). Secondary  
497 antibodies, goat-anti-mouse IgG, goat-anti-rabbit IgG were purchased from Jackson  
498 ImmunoResearch, goat-anti-mouse, Alexa Fluor 488, goat-anti-rabbit, Alexa Fluor 488,  
499 goat-anti-rabbit, Alexa Fluor 594, goat-anti-mouse, Alexa Fluor 555 and goat anti-rat,  
500 Alexa Fluor 555 from Invitrogen.

501 E64d and 3-MA were purchased from Sigma-Aldrich, EBSS from Gibco and  
502 AlamarBlue from Invitrogen. Cycloheximide (CHX) was a gift from Dr Jonathan  
503 Yewdell, NIAID, NIH (Bethesda, MD, USA).

504

#### 505 **Cell lines, plasmids and lentiviral or retroviral constructs**

506 DC2.4 (a kind gift from Dr Kenneth L Rock, University of Massachusetts Medical  
507 School, MA) [47], 293T, M2CK (MDCK cells stably express M2) [51] and X63-GM-  
508 CSF [77] cell lines were cultured in RF-10 (RPMI 1640 containing 10% fetal calf serum  
509 (FCS), 2-mercaptoethanol (2-ME) ( $5 \times 10^{-5}$  M), and antibiotics). For upregulating  
510 MHC-II expression, DC2.4 cells were pretreated with 1 ng/ml of IFN- $\gamma$  in RF-10 for  
511 24 h.

512 DC2.4-*Beclin1*<sup>-/-</sup>, DC2.4-*Atg7*<sup>-/-</sup> and DC2.4-*FgH1tUTG* cell lines were generated using  
513 CRISPR/Cas9 system [78]. Lentiviral particles were generated by transfection of  
514 FuCas9Cherry (Addgene#70182) along with packaging plasmids pMDL  
515 (Addgene#12551), pRSV-REV (Addgene#12553), and VSV-G (Addgene#12559)  
516 encoding lentiviral structural components into 293T cells for 48 h. DC2.4 cells were  
517 firstly transduced with FuCas9Cherry lentiviral supernatant containing 4  $\mu$ g/ml  
518 polybrene through spinning infection at 2500 rpm, 32°C for 2 h. After constructing the  
519 DC2.4-Cas9 cell line, the lentiviral particles containing mBeclin sgRNAs, mAtg7  
520 sgRNAs or FgH1tUTG empty vector (Addgene#70183, negative control) were  
521 generated from 293T cells with the same transfection method, then the DC2.4-Cas9  
522 cells were transduced by these lentiviruses as described above. The transduced cells  
523 were cloned *via* single cell sorting on a FACS ARIA III and cultured in RF-10  
524 containing 1 ng/ml doxycycline.

525 pBABE-puro-mCherry-EGFP-LC3B (Addgene#22418) is a retroviral based tandem  
526 report system for detecting autophagic flux [48]. Retroviral particles were generated by  
527 transfection LC3B plasmid along with packaging plasmids pCMV-Gag-Pol  
528 (Addgene#12263) and pCAG-Eco (Addgene#35617) encoding retroviral structural

529 components into 293T cells for 48 h. The DC2.4-mCherry-EGFP-LC3B cell line was  
530 generated with retroviral transduction.

531

### 532 **Mice**

533 Female C57BL/6 (B6) were purchased from the Walter Eliza Hall Institute of Medical  
534 Research animal facility (Kew, Melbourne, Australia). B6.Beclin1 conditional floxed  
535 mice (*Becn1*<sup>tm1a(KOMP)Wtsi</sup>) were purchased from genOway and crossed onto  
536 B6.ROSA26-CreERT2 mice [79] to generate the “BecConRosa” mouse strain. This  
537 enabled the ubiquitous deletion of the *Beclin1* gene following tamoxifen administration.  
538 B6.*Tap*<sup>-/-</sup> mice were a gift from Professor Luc van Kaer (School of Medicine,  
539 Vanderbilt University, Nashville, TN) [43]. Mice were bred under SPF conditions at  
540 La Trobe University. All animal experiments were approved by the La Trobe University  
541 Animal Ethics Committee and performed under the National Health and Medical  
542 Research Council of Australia guidelines.

543

### 544 **Bone-Marrow Derived Dendritic cells (BMDCs)**

545 For BMDC culture, 2 x 10<sup>6</sup> bone marrow cells collected from naive B6 mice,  
546 tamoxifen-induced B6.BecConRosa or control B6 mice were grown in a 10 cm petri  
547 dish (Corning) in 10 ml RF-10 containing 10% of X63-GM-CSF supernatant  
548 (containing-10 ng/ml granulocyte-macrophage-colony-stimulating factor, GM-CSF)  
549 [77]. Fresh culture medium (10 ml) was added on day 3 and day 6, respectively. On day  
550 8, non-adherent BMDCs were harvested.

551

### 552 **Antigen-specific T cell culture**

553 The primary CD8<sup>+</sup> T cell lines were established according to our published method [80].  
554 Briefly, splenic cells from IAV-infected memory mice were co-cultured with NP<sub>366-374</sub>-  
555 pulsed and irradiated-BMDCs. For establishing IAV-specific CD4<sup>+</sup> T cell line, CD8-  
556 depleted splenocytes were co-cultured with NP<sub>311-325</sub>- or PB2<sub>106-120</sub>-pulsed and

557 irradiated-BMDCs. All the cell lines were cultured in RF-10 supplement with 1X MEM  
558 NEAA (Gibco), 1X sodium pyruvate (Gibco) and hrIL-2 (10 unit/ml, PeproTech). The  
559 IAV specific CD4<sup>+</sup> and CD8<sup>+</sup> T cell lines were then re-stimulated by peptide-pul sed  
560 BMDCs regularly till high purity.

561

## 562 **Influenza A virus and infection**

563 Influenza A virus PR8 (A/Puerto Rico/8/34, H1N1) was obtained from Professor  
564 Lorena Brown (University of Melbourne, Australia). M2SR is a PR8 based, M2  
565 deletion mutant and prepared in M2CK cells (MDCK cells stably express PR8 M2) [51].  
566 X31 (A/X-31, H3N2) was obtained from Dr Jonathan Yewdell, NIAID, NIH (Bethesda,  
567 Maryland USA). PR8 and X-31 viruses were propagated in 10-day-old embryonated  
568 chicken eggs, titered and stored as previously described [81]. Virus stock was heat  
569 inactivated by incubation in a 65°C water bath for 1 h. For *in vitro* infection, cells were  
570 infected at multiplicity of infection (MOI) of 1 of PR8, M2SR or X31 for 1 h in 200 µl  
571 acidified RPMI-1640 medium, pH 6.8). RF-10 (2 ml) medium was then added, and the  
572 cells were cultured for 24 h in a 37°C incubator with 5% CO<sub>2</sub>. For *in vivo* infection,  
573 mice were intranasally infected with 100 pfu PR8 or 1000 pfu X31 (in 40 µl PBS).

574

## 575 **Preparation of rVV-infected P815 cell lysates**

576 P815 cells were infected with rVV-CR19 (negative control), or rVV-NP or rVV-PB2  
577 (kind gifts from Dr Jonathan Yewdell, NIAID, NIH, Bethesda, MD, USA) at a MOI of  
578 10 for 1 h at 37°C in 0.1% (w/v) BSA/PBS, followed by addition of 10 volumes of RF-  
579 10 medium followed by overnight incubation. Infected cells were pelleted and lysed  
580 with 8 M urea [15]. The lysates were aliquoted and stored at -20°C until use.

581

## 582 **Peptides, intracellular cytokine staining (ICS) and flow cytometry**

583 All the peptides were synthesized by Mimotopes (Clayton, Melbourne, Australia).

584 For *in vitro* ICS assays, BMDCs and/or DC2.4 cells were infected with PR8 (MOI = 1)  
585 or X31 (MOI = 1), or pulsed with PR8 NP protein (10 µg/ml, Sino Biological, Beijing,  
586 China) or pulsed with rVV-infected P815 lysate (40 µmol, 5 µl in volume, equivalent  
587 to 10<sup>5</sup> infected cells). After 24 h, these BMDCs were co-cultured with IAV-specific  
588 CD4<sup>+</sup> or CD8<sup>+</sup> T cell line for 5 h in the presence of 10 µg/ml brefeldin A (BFA). Cells  
589 were then stained for surface makers CD8 and CD4, fixed by 1% (v/v)  
590 paraformaldehyde (PFA), and subsequently stained for intracellular IFN-γ in PBS  
591 containing 0.2% (v/v) saponin [82]. Cells staining was analyzed on a FACSCanto II  
592 flow cytometer (BD Biosciences) or Cytoflex (Beckman), and data were analyzed with  
593 FlowJo software (FlowJo VX, Ashland, OR, USA).

594 For *ex vivo* ICS assay, bronchoalveolar lavage wash and spleens were harvested from  
595 mice 10-day post IAV infection. Cells were stimulated in RF-10 medium with 10<sup>-5</sup> M  
596 MHC-II-restricted peptides or 10<sup>-6</sup> M MHC-I-restricted peptides for 5 h in the presence  
597 of 10 µg/ml BFA. Intracellular cytokine staining for IFN-γ and data analysis were  
598 performed as described above.

599

## 600 **Western blotting**

601 For adherent cell lines, cell monolayers were washed twice with cold PBS and treated  
602 with RIPA lysis buffer (Sigma-Aldrich) on ice. For suspension cells, cells were washed  
603 twice in cold PBS, pelleted and lysed with RIPA buffer. Lysate protein concentration  
604 was quantified by a Bio-Rad protein assay kit (Bio-Rad). Equal amounts of samples (10  
605 µg) were separated on SDS-PAGE gels before being transferred onto nitrocellulose  
606 membranes (Thermo), incubated with primary and then corresponding secondary  
607 antibodies. The protein bands were visualized by an ECL Plus kit (GE Healthcare).

608

## 609 **Confocal microscopy**

610 DC2.4 cells infected with PR8 or X31 at MOI =1 for 24 h were washed with PBS and  
611 fixed with 4% (v/v) paraformaldehyde for 20 min at room temperature. Cell monolayers

612 were permeabilized with 0.2% (v/v) Triton X-100 for 10 min, blocked with PBS  
613 containing 5% bovine serum albumin (BSA) for 1 h at room temperature, and then  
614 incubated with primary antibodies (anti-LC3B, anti-Atg7, anti-Beclin1 anti-NP, anti-  
615 MHC-II or anti-H2-M) at 4 °C overnight, followed by 1 h incubation with secondary  
616 antibodies (goat-anti-rabbit 594, or goat-anti-mouse 488, or goat-anti-rat 555) at 37°C.  
617 The fluorescence signals were visualized with a Zeiss confocal fluorescence  
618 microscope 780 (Zeiss, German).

619

#### 620 **Author contributions**

621 Perform experiments: JD, CLu, CLiu and SO; Experimental design: WC and JD;  
622 Manuscript writing: JD and WC; Resources: WDF, EFL, PB and HP; Funding  
623 acquisition: WC.

624

#### 625 **Acknowledgements**

626 This project was supported by the NHMRC program grant 567122 to WC.

627

#### 628 **Declaration of interest**

629 PB is an employee of FluGen, the developer of the influenza vaccine candidate, M2SR.

630

#### 631 **References**

- 632 1. Sun, J. & Braciale, T. J. (2013) Role of T cell immunity in recovery from  
633 influenza virus infection, *Curr Opin Virol.* **3**, 425-9.
- 634 2. Bryant, P. & Ploegh, H. (2004) Class II MHC peptide loading by the professionals,  
635 *Curr Opin Immunol.* **16**, 96-102.
- 636 3. Neefjes, J., Jongma, M. L., Paul, P. & Bakke, O. (2011) Towards a systems  
637 understanding of MHC class I and MHC class II antigen presentation, *Nat Rev Immunol.*  
638 **11**, 823-36.
- 639 4. Cresswell, P., Ackerman, A. L., Giodini, A., Peaper, D. R. & Wearsch, P. A.

- 640 (2005) Mechanisms of MHC class I-restricted antigen processing and cross-presentation,  
641 *Immunol Rev.* **207**, 145-57.
- 642 5. Heath, W. R. & Carbone, F. R. (2001) Cross-presentation, dendritic cells,  
643 tolerance and immunity, *Annu Rev Immunol.* **19**, 47-64.
- 644 6. Zhou, D., Li, P., Lin, Y., Lott, J. M., Hislop, A. D., Canaday, D. H., Brutkiewicz,  
645 R. R. & Blum, J. S. (2005) Lamp-2a facilitates MHC class II presentation of  
646 cytoplasmic antigens, *Immunity.* **22**, 571-81.
- 647 7. Zeng, G., Wang, X., Robbins, P. F., Rosenberg, S. A. & Wang, R. F. (2001) CD4(+)  
648 T cell recognition of MHC class II-restricted epitopes from NY-ESO-1 presented by a  
649 prevalent HLA DP4 allele: association with NY-ESO-1 antibody production, *Proc Natl*  
650 *Acad Sci U S A.* **98**, 3964-9.
- 651 8. Dissanayake, S. K., Tuera, N. & Ostrand-Rosenberg, S. (2005) Presentation of  
652 endogenously synthesized MHC class II-restricted epitopes by MHC class II cancer  
653 vaccines is independent of transporter associated with Ag processing and the  
654 proteasome, *J Immunol.* **174**, 1811-9.
- 655 9. Thompson, J. A., Srivastava, M. K., Bosch, J. J., Clements, V. K., Ksander, B.  
656 R. & Ostrand-Rosenberg, S. (2008) The absence of invariant chain in MHC II cancer  
657 vaccines enhances the activation of tumor-reactive type 1 CD4+ T lymphocytes, *Cancer*  
658 *Immunol Immunother.* **57**, 389-98.
- 659 10. Jaraquemada, D., Marti, M. & Long, E. O. (1990) An endogenous processing pathway  
660 in vaccinia virus-infected cells for presentation of cytoplasmic antigens to class  
661 II-restricted T cells, *J Exp Med.* **172**, 947-54.
- 662 11. Miller, M. A., Ganesan, A. P., Luckashenak, N., Mendonca, M. & Eisenlohr, L. C.  
663 (2015) Endogenous antigen processing drives the primary CD4+ T cell response to  
664 influenza, *Nat Med.* **21**, 1216-22.
- 665 12. Chen, M., Shirai, M., Liu, Z., Arichi, T., Takahashi, H. & Nishioka, M. (1998)  
666 Efficient class II major histocompatibility complex presentation of endogenously  
667 synthesized hepatitis C virus core protein by Epstein-Barr virus-transformed B-

668 lymphoblastoid cell lines to CD4(+) T cells, *Journal of virology*. **72**, 8301-8.

669 13. Gueguen, M. & Long, E. O. (1996) Presentation of a cytosolic antigen by major  
670 histocompatibility complex class II molecules requires a long-lived form of the  
671 antigen, *Proc Natl Acad Sci U S A*. **93**, 14692-7.

672 14. Schmid, D., Pypaert, M. & Munz, C. (2007) Antigen-loading compartments for major  
673 histocompatibility complex class II molecules continuously receive input from  
674 autophagosomes, *Immunity*. **26**, 79-92.

675 15. Chen, L., Zanker, D., Xiao, K., Wu, C., Zou, Q. & Chen, W. (2014) Immunodominant  
676 CD4+ T-cell responses to influenza A virus in healthy individuals focus on matrix 1  
677 and nucleoprotein, *Journal of virology*. **88**, 11760-73.

678 16. Dengjel, J., Schoor, O., Fischer, R., Reich, M., Kraus, M., Muller, M., Kreyborg,  
679 K., Altenberend, F., Brandenburg, J., Kalbacher, H., Brock, R., Driessen, C.,  
680 Rammensee, H. G. & Stevanovic, S. (2005) Autophagy promotes MHC class II presentation  
681 of peptides from intracellular source proteins, *Proc Natl Acad Sci U S A*. **102**,  
682 7922-7.

683 17. Nimmerjahn, F., Milosevic, S., Behrends, U., Jaffee, E. M., Pardoll, D. M.,  
684 Bornkamm, G. W. & Mautner, J. (2003) Major histocompatibility complex class II-  
685 restricted presentation of a cytosolic antigen by autophagy, *Eur J Immunol*. **33**,  
686 1250-9.

687 18. Duraes, F. V., Niven, J., Dubrot, J., Hugues, S. & Gannage, M. (2015)  
688 Macroautophagy in Endogenous Processing of Self- and Pathogen-Derived Antigens for  
689 MHC Class II Presentation, *Front Immunol*. **6**, 459.

690 19. Paludan, C., Schmid, D., Landthaler, M., Vockerodt, M., Kube, D., Tuschl, T. &  
691 Munz, C. (2005) Endogenous MHC class II processing of a viral nuclear antigen after  
692 autophagy, *Science*. **307**, 593-596.

693 20. Coulon, P. G., Richetta, C., Rouers, A., Blanchet, F. P., Urrutia, A., Guerbois,  
694 M., Piguet, V., Theodorou, I., Bet, A., Schwartz, O., Tangy, F., Graff-Dubois, S.,  
695 Cardinaud, S. & Moris, A. (2016) HIV-Infected Dendritic Cells Present Endogenous MHC

696 Class II-Restricted Antigens to HIV-Specific CD4+ T Cells, *J Immunol.* **197**, 517-32.

697 21. Taubenberger, J. K. & Kash, J. C. (2010) Influenza Virus Evolution, Host  
698 Adaptation, and Pandemic Formation, *Cell Host & Microbe.* **7**, 440-451.

699 22. Flannery, B., Chung, J. R., Monto, A. S., Martin, E. T., Belongia, E. A.,  
700 McLean, H. Q., Gaglani, M., Murthy, K., Zimmerman, R. K., Nowalk, M. P., Jackson, M.  
701 L., Jackson, L. A., Rolfes, M. A., Spencer, S., Fry, A. M. & Investigators, U. S. F.  
702 V. (2019) Influenza Vaccine Effectiveness in the United States During the 2016-2017  
703 Season, *Clin Infect Dis.* **68**, 1798-1806.

704 23. Blyth, C. C., Macartney, K. K., McRae, J., Clark, J. E., Marshall, H. S.,  
705 Buttery, J., Francis, J. R., Kotsimbos, T., Kelly, P. M., Cheng, A. C., Paediatric  
706 Active Enhanced Disease, S. & Influenza Complications Alert Network, C. (2019)  
707 Influenza Epidemiology, Vaccine Coverage and Vaccine Effectiveness in Children  
708 Admitted to Sentinel Australian Hospitals in 2017: Results from the PAEDS-FluCAN  
709 Collaboration, *Clin Infect Dis.* **68**, 940-948.

710 24. Fielding, J. E., Levy, A., Chilver, M. B., Deng, Y. M., Regan, A. K., Grant, K.  
711 A., Stocks, N. P. & Sullivan, S. G. (2016) Effectiveness of seasonal influenza  
712 vaccine in Australia, 2015: An epidemiological, antigenic and phylogenetic assessment,  
713 *Vaccine.* **34**, 4905-4912.

714 25. Talbot, T. R., Crocker, D. D., Peters, J., Doersam, J. K., Ikizler, M. R.,  
715 Sannella, E., Wright, P. E. & Edwards, K. M. (2005) Duration of virus shedding after  
716 trivalent intranasal live attenuated influenza vaccination in adults, *Infect Control*  
717 *Hosp Epidemiol.* **26**, 494-500.

718 26. Tamura, S. I. & Kurata, T. (2004) Defense mechanisms against influenza virus  
719 infection in the respiratory tract mucosa, *Jpn J Infect Dis.* **57**, 236-247.

720 27. Sycheva, A. L., Pogorelyy, M. V., Komech, E. A., Minervina, A. A., Zvyagin, I.  
721 V., Staroverov, D. B., Chudakov, D. M., Lebedev, Y. B. & Mamedov, I. Z. (2018)  
722 Quantitative profiling reveals minor changes of T cell receptor repertoire in  
723 response to subunit inactivated influenza vaccine, *Vaccine.* **36**, 1599-1605.

- 724 28. Hoft, D. F., Lottenbach, K. R., Blazevic, A., Turan, A., Blevins, T. P., Pacatte,  
725 T. P., Yu, Y., Mitchell, M. C., Hoft, S. G. & Belshe, R. B. (2017) Comparisons of  
726 the Humoral and Cellular Immune Responses Induced by Live Attenuated Influenza  
727 Vaccine and Inactivated Influenza Vaccine in Adults, *Clin Vaccine Immunol.* **24**.
- 728 29. Cox, R. J., Brokstad, K. A. & Ogra, P. (2004) Influenza virus: immunity and  
729 vaccination strategies. Comparison of the immune response to inactivated and live,  
730 attenuated influenza vaccines, *Scand J Immunol.* **59**, 1-15.
- 731 30. Sridhar, S., Brokstad, K. A. & Cox, R. J. (2015) Influenza Vaccination Strategies:  
732 Comparing Inactivated and Live Attenuated Influenza Vaccines, *Vaccines (Basel).* **3**,  
733 373-89.
- 734 31. Reggiori, F. (2006) 1. Membrane origin for autophagy, *Curr Top Dev Biol.* **74**,  
735 1-30.
- 736 32. Yorimitsu, T. & Klionsky, D. J. (2005) Autophagy: molecular machinery for self-  
737 eating, *Cell Death Differ.* **12 Suppl 2**, 1542-52.
- 738 33. Klionsky, D. J. (2007) Autophagy: from phenomenology to molecular understanding  
739 in less than a decade, *Nat Rev Mol Cell Bio.* **8**, 931-937.
- 740 34. Wang, R. F., Zhu, Y. X., Zhao, J. C., Ren, C. W., Li, P., Chen, H. C., Jin, M.  
741 L. & Zhou, H. B. (2019) Autophagy Promotes Replication of Influenza A Virus In Vitro,  
742 *Journal of virology.* **93**.
- 743 35. Zhou, Z., Jiang, X., Liu, D., Fan, Z., Hu, X., Yan, J., Wang, M. & Gao, G. F.  
744 (2009) Autophagy is involved in influenza A virus replication, *Autophagy.* **5**, 321-8.
- 745 36. Gannage, M., Dormann, D., Albrecht, R., Dengjel, J., Torossi, T., Ramer, P. C.,  
746 Lee, M., Strowig, T., Arrey, F., Conenello, G., Pypaert, M., Andersen, J., Garcia-  
747 Sastre, A. & Munz, C. (2009) Matrix protein 2 of influenza A virus blocks  
748 autophagosome fusion with lysosomes, *Cell Host Microbe.* **6**, 367-80.
- 749 37. Ren, Y., Li, C., Feng, L., Pan, W., Li, L., Wang, Q., Li, J., Li, N., Han, L.,  
750 Zheng, X., Niu, X., Sun, C. & Chen, L. (2016) Proton Channel Activity of Influenza  
751 A Virus Matrix Protein 2 Contributes to Autophagy Arrest, *Journal of virology.* **90**,

752 591-8.

753 38. Comber, J. D., Robinson, T. M., Siciliano, N. A., Snook, A. E. & Eisenlohr, L.  
754 C. (2011) Functional Macroautophagy Induction by Influenza A Virus without a  
755 Contribution to Major Histocompatibility Complex Class II-Restricted Presentation,  
756 *Journal of virology*. **85**, 6453-6463.

757 39. Crowe, S. R., Miller, S. C., Brown, D. M., Adams, P. S., Dutton, R. W., Harmsen,  
758 A. G., Lund, F. E., Randall, T. D., Swain, S. L. & Woodland, D. L. (2006) Uneven  
759 distribution of MHC class II epitopes within the influenza virus, *Vaccine*. **24**, 457-  
760 467.

761 40. Zanker, D., Waithman, J., Yewdell, J. W. & Chen, W. (2013) Mixed proteasomes  
762 function to increase viral peptide diversity and broaden antiviral CD8+ T cell  
763 responses, *J Immunol*. **191**, 52-9.

764 41. Santana, S., Bullido, M. J., Recuero, M., Valdivieso, F. & Aldudo, J. (2012)  
765 Herpes simplex virus type I induces an incomplete autophagic response in human  
766 neuroblastoma cells, *J Alzheimers Dis*. **30**, 815-31.

767 42. Guermontprez, P., Saveanu, L., Kleijmeer, M., Davoust, J., van Endert, P. &  
768 Amigorena, S. (2003) ER-phagosome fusion defines an MHC class I cross-presentation  
769 compartment in dendritic cells, *Nature*. **425**, 397-402.

770 43. Van Kaer, L., Ashton-Rickardt, P. G., Ploegh, H. L. & Tonegawa, S. (1992) TAP1  
771 mutant mice are deficient in antigen presentation, surface class I molecules, and  
772 CD4-8+ T cells, *Cell*. **71**, 1205-14.

773 44. Klionsky, D. J., Cuervo, A. M. & Seglen, P. O. (2007) Methods for monitoring  
774 autophagy from yeast to human, *Autophagy*. **3**, 181-206.

775 45. Mizushima, N., Yoshimori, T. & Ohsumi, Y. (2011) The Role of Atg Proteins in  
776 Autophagosome Formation, *Annu Rev Cell Dev Bi*. **27**, 107-132.

777 46. Mizushima, N. & Yoshimori, T. (2007) How to interpret LC3 immunoblotting,  
778 *Autophagy*. **3**, 542-545.

779 47. Shen, Z. H., Reznikoff, G., Dranoff, G. & Rock, K. L. (1997) Cloned dendritic

780 cells can present exogenous antigens on both MHC class I and class II molecules, *J*  
781 *Immunol.* **158**, 2723–2730.

782 48. N’Diaye, E. N., Kajihara, K. K., Hsieh, I., Morisaki, H., Debnath, J. & Brown,  
783 E. J. (2009) PLIC proteins or ubiquilins regulate autophagy-dependent cell survival  
784 during nutrient starvation, *Embo Rep.* **10**, 173–9.

785 49. Munafò, D. B. & Colombo, M. I. (2001) A novel assay to study autophagy:  
786 regulation of autophagosome vacuole size by amino acid deprivation, *J Cell Sci.* **114**,  
787 3619–29.

788 50. Martinet, W., De Meyer, G. R., Andries, L., Herman, A. G. & Kockx, M. M. (2006)  
789 In situ detection of starvation-induced autophagy, *J Histochem Cytochem.* **54**, 85–96.

790 51. Sarawar, S., Hatta, Y., Watanabe, S., Dias, P., Neumann, G., Kawaoka, Y. &  
791 Bilsel, P. (2016) M2SR, a novel live single replication influenza virus vaccine,  
792 provides effective heterosubtypic protection in mice, *Vaccine.* **34**, 5090–5098.

793 52. Danielian, P. S., White, R., Hoare, S. A., Fawell, S. E. & Parker, M. G. (1993)  
794 Identification of Residues in the Estrogen-Receptor That Confer Differential  
795 Sensitivity to Estrogen and Hydroxytamoxifen, *Mol Endocrinol.* **7**, 232–240.

796 53. Littlewood, T. D., Hancock, D. C., Danielian, P. S., Parker, M. G. & Even, G.  
797 I. (1995) A Modified Estrogen-Receptor Ligand-Binding Domain as an Improved Switch  
798 for the Regulation of Heterologous Proteins, *Nucleic Acids Res.* **23**, 1686–1690.

799 54. McLellan, M. A., Rosenthal, N. A. & Pinto, A. R. (2017) Cre-loxP-Mediated  
800 Recombination: General Principles and Experimental Considerations, *Curr Protoc Mouse*  
801 *Biol.* **7**, 1–12.

802 55. Kang, R., Zeh, H. J., Lotze, M. T. & Tang, D. (2011) The Beclin 1 network  
803 regulates autophagy and apoptosis, *Cell Death and Differentiation.* **18**, 571–580.

804 56. Liang, C., Lee, J. S., Inn, K. S., Gack, M. U., Li, Q., Roberts, E. A., Vergne,  
805 I., Deretic, V., Feng, P., Akazawa, C. & Jung, J. U. (2008) Beclin1-binding UVRAG  
806 targets the class C Vps complex to coordinate autophagosome maturation and endocytic  
807 trafficking, *Nat Cell Biol.* **10**, 776–87.

- 808 57. Kim, H. J., Zhong, Q., Sheng, Z. H., Yoshimori, T., Liang, C. & Jung, J. U.  
809 (2012) Beclin-1-interacting autophagy protein Atg14L targets the SNARE-associated  
810 protein Snapin to coordinate endocytic trafficking, *J Cell Sci.* **125**, 4740-50.
- 811 58. Xiong, J. H. (2015) Atg7 in development and disease: panacea or Pandora's Box?,  
812 *Protein Cell.* **6**, 722-734.
- 813 59. Eggensperger, S. & Tampe, R. (2015) The transporter associated with antigen  
814 processing: a key player in adaptive immunity, *Biol Chem.* **396**, 1059-72.
- 815 60. Cresswell, P. (1994) Assembly, Transport, and Function of Mhc Class-II Molecules,  
816 *Annual Review of Immunology.* **12**, 259-293.
- 817 61. Gannage, M. & Munz, C. (2009) Autophagy in MHC class II presentation of  
818 endogenous antigens, *Curr Top Microbiol Immunol.* **335**, 123-40.
- 819 62. Petiot, A., Ogier-Denis, E., Blommaart, E. F., Meijer, A. J. & Codogno, P.  
820 (2000) Distinct classes of phosphatidylinositol 3'-kinases are involved in signaling  
821 pathways that control macroautophagy in HT-29 cells, *J Biol Chem.* **275**, 992-8.
- 822 63. Yang, Y. P., Hu, L. F., Zheng, H. F., Mao, C. J., Hu, W. D., Xiong, K. P., Wang,  
823 F. & Liu, C. F. (2013) Application and interpretation of current autophagy inhibitors  
824 and activators, *Acta Pharmacol Sin.* **34**, 625-35.
- 825 64. Wu, Y., Wang, X., Guo, H., Zhang, B., Zhang, X. B., Shi, Z. J. & Yu, L. (2013)  
826 Synthesis and screening of 3-MA derivatives for autophagy inhibitors, *Autophagy.* **9**,  
827 595-603.
- 828 65. Hwang, K. E., Kim, Y. S., Jung, J. W., Kwon, S. J., Park, D. S., Cha, B. K.,  
829 Oh, S. H., Yoon, K. H., Jeong, E. T. & Kim, H. R. (2015) Inhibition of autophagy  
830 potentiates pemetrexed and simvastatin-induced apoptotic cell death in malignant  
831 mesothelioma and non-small cell lung cancer cells, *Oncotarget.* **6**, 29482-96.
- 832 66. Ni, H. M., Bockus, A., Wozniak, A. L., Jones, K., Weinman, S., Yin, X. M. &  
833 Ding, W. X. (2011) Dissecting the dynamic turnover of GFP-LC3 in the autolysosome,  
834 *Autophagy.* **7**, 188-204.
- 835 67. Ariaans, M. P., van de Haar, P. M., Lowenthal, J. W., van Eden, W., Hensen, E.

- 836 J. & Vervelde, L. (2008) ELISPOT and intracellular cytokine staining: novel assays  
837 for quantifying T cell responses in the chicken, *Dev Comp Immunol.* **32**, 1398-404.
- 838 68. Doherty, P. C., Brown, L. E., Kelso, A. & Thomas, P. G. (2009) Immunity to avian  
839 influenza A viruses, *Rev Sci Tech.* **28**, 175-85.
- 840 69. van de Sandt, C. E., Kreijtz, J. H. & Rimmelzwaan, G. F. (2012) Evasion of  
841 influenza A viruses from innate and adaptive immune responses, *Viruses.* **4**, 1438-76.
- 842 70. Basha, S., Hazenfeld, S., Brady, R. C. & Subbramanian, R. A. (2011) Comparison  
843 of antibody and T-cell responses elicited by licensed inactivated- and live-  
844 attenuated influenza vaccines against H3N2 hemagglutinin, *Hum Immunol.* **72**, 463-9.
- 845 71. Rajao, D. S. & Perez, D. R. (2018) Universal Vaccines and Vaccine Platforms to  
846 Protect against Influenza Viruses in Humans and Agriculture, *Front Microbiol.* **9**.
- 847 72. Blanco-Lobo, P., Nogales, A., Rodriguez, L. & Martinez-Sobrido, L. (2019) Novel  
848 Approaches for The Development of Live Attenuated Influenza Vaccines, *Viruses.* **11**.
- 849 73. Hatta, Y., Boltz, D., Sarawar, S., Kawaoka, Y., Neumann, G. & Bilsel, P. (2017)  
850 M2SR, a novel live influenza vaccine, protects mice and ferrets against highly  
851 pathogenic avian influenza, *Vaccine.* **35**, 4177-4183.
- 852 74. Hosseini, S., Wilk, E., Michaelsen-Preusse, K., Gerhauser, I., Baumgartner, W.,  
853 Geffers, R., Schughart, K. & Korte, M. (2018) Long-Term Neuroinflammation Induced by  
854 Influenza A Virus Infection and the Impact on Hippocampal Neuron Morphology and  
855 Function, *J Neurosci.* **38**, 3060-3080.
- 856 75. Ye, Z. P., Pal, R., Fox, J. W. & Wagner, R. R. (1987) Functional and antigenic  
857 domains of the matrix (M1) protein of influenza A virus, *Journal of virology.* **61**,  
858 239-46.
- 859 76. Fu, T. M., Freed, D. C., Horton, M. S., Fan, J., Citron, M. P., Joyce, J. G.,  
860 Garsky, V. M., Casimiro, D. R., Zhao, Q., Shiver, J. W. & Liang, X. (2009)  
861 Characterizations of four monoclonal antibodies against M2 protein ectodomain of  
862 influenza A virus, *Virology.* **385**, 218-26.
- 863 77. Stockinger, B., Zal, T., Zal, A. & Gray, D. (1996) B cells solicit their own

864 help from T cells, *J Exp Med.* **183**, 891–9.

865 78. Aubrey, B. J., Kelly, G. L., Kueh, A. J., Brennan, M. S., O'Connor, L., Milla,  
866 L., Wilcox, S., Tai, L., Strasser, A. & Herold, M. J. (2015) An Inducible Lentiviral  
867 Guide RNA Platform Enables the Identification of Tumor-Essential Genes and Tumor-  
868 Promoting Mutations In Vivo, *Cell Rep.* **10**, 1422–1432.

869 79. Seibler, J., Zevnik, B., Kuter-Luks, B., Andreas, S., Kern, H., Hennek, T.,  
870 Rode, A., Heimann, C., Faust, N., Kauselmann, G., Schoor, M., Jaenisch, R., Rajewsky,  
871 K., Kuhn, R. & Schwenk, F. (2003) Rapid generation of inducible mouse mutants,  
872 *Nucleic Acids Res.* **31**, e12.

873 80. Zanker, D., Xiao, K., Oveissi, S., Guillaume, P., Luescher, I. F. & Chen, W.  
874 (2013) An optimized method for establishing high purity murine CD8<sup>+</sup> T cell cultures,  
875 *J Immunol Methods.* **387**, 173–80.

876 81. Chen, W. S., Calvo, P. A., Malide, D., Gibbs, J., Schubert, U., Bacik, I.,  
877 Basta, S., O'Neill, R., Schickli, J., Palese, P., Henklein, P., Bennink, J. R. &  
878 Yewdell, J. W. (2001) A novel influenza A virus mitochondrial protein that induces  
879 cell death, *Nature Medicine.* **7**, 1306–1312.

880 82. Chen, W., Anton, L. C., Bennink, J. R. & Yewdell, J. W. (2000) Dissecting the  
881 multifactorial causes of immunodominance in class I-restricted T cell responses to  
882 viruses, *Immunity.* **12**, 83–93.

883

884

## 885 **Figure legends**

### 886 **Figure 1. Endogenous IAV antigen presentation by MHC-II.**

887 (A) B6 mice were intranasally infected with 100 pfu of PR8, the CD4<sup>+</sup> T cell response  
888 in the BAL or spleen of IAV-infected mice were assessed using 17 MHC-II-restricted  
889 peptides on 10 dpi *via* standard ICS assay. NIL indicates no peptide addition. (B) NP<sub>311-</sub>  
890 <sub>325</sub>-specific CD4<sup>+</sup> T cell line and NP<sub>366-374</sub>-specific CD8<sup>+</sup> T cell line were stimulated by  
891 NP<sub>311-325</sub> and NP<sub>366-374</sub> peptides, respectively, at various peptide concentrations in the

892 presence of BFA for 5 h. Error bars indicate the  $\pm$  SEM of 5 independent experiments  
893 (n=5). (C) Endogenous IAV antigen presentation was assessed by PR8 infected  
894 BMDCs (MOI=1, 24hpi). Infected-BMDCs were then co-cultured with NP<sub>311-325</sub>-  
895 specific CD4<sup>+</sup> T cells and NP<sub>366-374</sub>-specific CD8<sup>+</sup> T cells in the presence of BFA for 5  
896 h. (D) BMDCs infected with PR8 (MOI=1, 24h), inactivated-PR8 (65°C for 1 h, MOI=1,  
897 24h), pulsed with exogenous NP (10  $\mu$ g/ml, 24h) or pulsed with heated-NP (65°C for 1  
898 h, 10  $\mu$ g/ml, 24h). These APCs were then co-cultured with NP<sub>311-325</sub>-specific CD4<sup>+</sup> or  
899 NP<sub>366-374</sub>-specific CD8<sup>+</sup> T cells in the presence of BFA for 5 h. (E) BMDCs were  
900 pretreated with or without 25  $\mu$ g/ml CHX for 20 min before being infected with PR8  
901 (MOI=1) and for further 24 h before being co-cultured with NP<sub>311-325</sub>-specific CD4<sup>+</sup> T  
902 cells in the presence of BFA for 5 h. (F) BMDCs infected with PR8 at MOI=1 were  
903 treated with or without 10  $\mu$ g/ml BFA for further 24 h before being co-cultured with  
904 NP<sub>311-325</sub>-specific CD4<sup>+</sup> T cells in the presence of BFA for 5 h. The IFN- $\gamma$  productions  
905 in the above experiments were detected by standard ICS assays (APCs: T=2:1), and  
906 IFN- $\gamma$ <sup>+</sup> T cells were expressed as a percentage of total CD4<sup>+</sup> or total CD8<sup>+</sup> T cells,  
907 respectively. Experiments were performed twice with similar results (A, D, E, F; n=2).  
908

909 **Figure 2. Endogenous IAV antigen presentation by MHC-II *in vitro* is epitope-**  
910 **dependent.**

911 (A) NP<sub>311-325</sub>-specific CD4<sup>+</sup> T cells (B) PB2<sub>106-120</sub>-specific CD4<sup>+</sup> T cells were co-  
912 cultured with PR8-infected BMDCs, or relevant rVV lysate-pulsed BMDCs in the  
913 presence of BFA for 5 h (APCs: T=2:1). (C) NP<sub>311-325</sub>-specific CD4<sup>+</sup> T cells or (D)  
914 PB2<sub>106-120</sub>-specific CD4<sup>+</sup> T cells were stimulated by NP<sub>311-325</sub> peptide or PB2<sub>106-120</sub>  
915 peptide, respectively, at various peptide concentrations in the presence of BFA for 5 h.  
916 IFN- $\gamma$  production was detected by standard ICS assay, and IFN- $\gamma$ <sup>+</sup> CD4<sup>+</sup> T cells were  
917 expressed as a percentage of total CD4<sup>+</sup> T cells. Experiments were performed twice  
918 with similar results (A, B, C, D; n=2).

919

920 **Figure 3. Endogenous IAV antigen presentation by MHC-II is reduced by**  
921 **functional TAP.**

922 (A) WT BMDCs or *Tap1*<sup>-/-</sup> BMDCs were infected with PR8 (MOI=1) or X31 (MOI=1).  
923 24 hpi, the IAV-infected APCs were co-cultured with NP<sub>366-374</sub>-specific CD8<sup>+</sup> or NP<sub>311-</sub>  
924 <sub>325</sub>-specific CD4<sup>+</sup> T cells in the presence of BFA for 5 h (APCs: T=2:1). IFN- $\gamma$   
925 production was detected by standard ICS assays, and IFN- $\gamma$ <sup>+</sup> T cells were expressed as  
926 a percentage of total CD4<sup>+</sup> or total CD8<sup>+</sup> T cells. Error bars indicate the  $\pm$  SEM of  
927 experimental replicates. Two independent experiments were performed with similar  
928 results, and each independent experiment included 3 biological replicates (n=6). \**P* <  
929 0.05; \*\**P* < 0.01; \*\*\**P* < 0.001; \*\*\*\**P* < 0.0001 and ns *P* > 0.05 (determined by  
930 unpaired two-tailed Student's *t*-test). (B) WT B6 mice and B6.*Tap1*<sup>-/-</sup> mice were  
931 infected with 1000 pfu of X31. Antigen-specific T cells in the BAL washes were  
932 assessed using 17 MHC-II-restricted peptides and 4 MHC-I-restricted peptides *via*  
933 standard ICS assays at 10 dpi. IFN- $\gamma$ <sup>+</sup> T cells were expressed as a percentage of total  
934 CD4<sup>+</sup> or total CD8<sup>+</sup> T cells. NIL indicates no peptide addition. Error bars indicate  
935  $\pm$ SEM of 3 mice per group. Experiments were performed twice with similar results  
936 (n=6). (C) Spleen T cell phenotypes of WT B6 and B6.*Tap1*<sup>-/-</sup> mice (n=3).

937

938 **Figure 4. IAV infection induces autophagosome accumulation in dendritic cells.**

939 (A) BMDCs or (B) DC2.4 cells were mock-infected or infected with PR8 or X31 for 6,  
940 12 and 24 h. At the end of the infection, the expression levels of Atg7, Beclin1, p62,  
941 M1, LC3 and GAPDH (loading control) were analyzed by western blotting.  
942 Experiments were performed 3 times (n=3) with similar results. (C) DC2.4 cells were  
943 mock-infected or infected with PR8 or X31. At 24 hpi, the cells were fixed and then  
944 assessed by indirect immunofluorescence using antibodies against Beclin1, Atg7 or  
945 LC3, respectively, followed by the corresponding secondary antibody conjugated to  
946 FITC. The cell nucleuses were stained by DAPI. The fluorescent signals were  
947 visualized by confocal microscopy, scale bar: 10  $\mu$ m. The fluorescence intensity of

948 Beclin1, Atg7 and LC3 in each group was graphed on the right side. Error bars indicate  
949 the  $\pm$  SEM of 60 cells per group from two independent experiments (n=60). \* $P < 0.05$ ;  
950 \*\* $P < 0.01$ ; \*\*\* $P < 0.001$ ; \*\*\*\* $P < 0.0001$  and ns  $P > 0.05$  (determined by one-way  
951 ANOVA followed by a Dunnett test). (D) DC2.4 cells were treated with or without  
952 EBSS for 24 h and the expression levels of p62, LC3 and GAPDH (loading control)  
953 were analyzed by western blotting. (E) DC2.4-mCherry-EGFP-LC3B cells were mock-  
954 infected, infected with PR8 or X31, or treated with EBSS for 24 h. Cells were analyzed  
955 by flow cytometry for GFP and mCherry fluorescence intensity. (F) DC2.4 cells were  
956 PR8-infected or M2SR-infected for 6, 12, or 24 h (MOI=1). The expression levels of  
957 p62, M1, LC3, M2 and GAPDH (loading control) were analyzed by western blotting.  
958 (G) DC2.4-mCherry-EGFP-LC3B cells were mock-infected, infected with PR8 or  
959 M2SR, or treated with EBSS for 24 h. Cells were analyzed by flow cytometry for GFP  
960 and mCherry fluorescence intensity. Experiments were performed 3 times with similar  
961 results (D, E, F, G; n=3)

962

963 **Figure 5. Autophagy inhibitors downregulate endogenous IAV antigen**  
964 **presentation by MHC-II.**

965 (A) BMDCs were infected with PR8 or X31 in the presence or absence of 3-MA (5  
966 mM) or E64d (10  $\mu$ g/ml). At 24 hpi, cell lysates were prepared and analyzed by western  
967 blotting using anti-LC3, anti-p62, anti-M1 and anti-GAPDH (loading control). (B) The  
968 cell viability of BMDCs or DC2.4 cells were detected by AlamarBlue kit at 24 h after  
969 cells were treated by control, 3-MA or E64d. Error bars indicate  $\pm$  SD of 5 biological  
970 replicates (n=5) per group. Experiments were performed twice with similar results. (C)  
971 BMDCs were infected with PR8 or X31, or mock infected, in the presence or absence  
972 of 3-MA or E64d. At 24 hpi, endogenous IAV antigen presentation by these BMDCs  
973 were assessed with NP<sub>311-325</sub>-specific CD4<sup>+</sup> T cells in the presence of BFA for 5 h  
974 (APCs: T=2:1) and revealed by standard ICS assays. IFN- $\gamma$ <sup>+</sup> T cells were expressed as  
975 a percentage of total CD4<sup>+</sup> T cells. (D) Virus infection efficiency and the MFI of

976 infected BMDCs described in (C) were assessed by IAV NP expression *via* flow  
977 cytometry. (E) DC2.4 cells were infected and their endogenous IAV antigen  
978 presentation (E) and virus infection efficiency and the MFI of infected DC2.4 cells (F)  
979 as described in (C and E). Error bars indicate  $\pm$  SEM of experimental replicates. Similar  
980 results were obtained from two independent experiments with 3 biological replicates  
981 (C, D, E, F; n=6). \* $P < 0.05$ ; \*\* $P < 0.01$ ; \*\*\* $P < 0.001$ ; \*\*\*\* $P < 0.0001$  and ns  $P >$   
982 0.05 (determined by one-way ANOVA followed by a Dunnett test). NA means not  
983 available.

984

985 **Figure 6. Autophagy-related gene *Beclin1* contributes to endogenous IAV antigen**  
986 **presentation by MHC-II.**

987 (A) *In vitro* cultured BMDCs from tamoxifen-treated B6 or B6.BecConRosa mice were  
988 assessed for Beclin1 and GAPDH (loading control) expression by western blotting.  
989 Experiments were performed 3 times (n=3) with similar results. (B) BMDCs in (A)  
990 were mock infected or infected with PR8 or X31. At 24 hpi, virus infection efficiency  
991 and the MFI of infected BMDCs were assessed by IAV NP expression *via* flow  
992 cytometry. (C) Endogenous antigen presentation by BMDCs described in (B) was  
993 assessed by NP<sub>311-325</sub>-specific CD4<sup>+</sup> T cells *via* standard ICS assays (APCs: T=2:1).  
994 Error bars indicate  $\pm$ SEM of the experimental replicates. Two independent experiments  
995 were performed with similar results, and each independent experiment included 3  
996 biological replicates (B, C; n=6). \* $P < 0.05$ ; \*\* $P < 0.01$ ; \*\*\* $P < 0.001$ ; \*\*\*\* $P < 0.0001$   
997 and ns  $P > 0.05$  (determined by one-way ANOVA followed by a Dunnett test). NA  
998 means not available.

999

1000 **Figure 7. Not only *Beclin1* but also *Atg7* contributes to endogenous IAV antigen**  
1001 **presentation by MHC-II.**

1002 (A) Knockout DC2.4 cell lines were confirmed by western blotting for lack of the  
1003 targeted protein expression. Experiments were performed 3 times (n=3) with similar

1004 results. (B) DC2.4-*Beclin1*<sup>-/-</sup> knockout status was confirmed by Sanger sequencing. A  
1005 part of cDNA sequence and its amino acid sequence translated from related cDNA  
1006 between WT DC2.4 cells and DC2.4-*Beclin1*<sup>-/-</sup> cells were displayed. (C) DC2.4-*Atg7*<sup>-/-</sup>  
1007 knockout status was confirmed by Sanger sequencing. A part of cDNA sequence and  
1008 its amino acid sequence translated from related cDNA between WT DC2.4 cells and  
1009 DC2.4-*Atg7*<sup>-/-</sup> cells were displayed. (D) DC2.4-*FgH1tUTG* (control), DC2.4-*Beclin1*<sup>-/-</sup>,  
1010 and DC2.4-*Atg7*<sup>-/-</sup> cells were mock infected or infected with PR8 or X31. At 24 hpi,  
1011 virus infection efficiency and the MFI of infected DC2.4 cells were assessed by IAV  
1012 NP expression *via* flow cytometry. (E) Endogenous antigen presentation by DC2.4 cells  
1013 treated as described in (E) was assessed by NP<sub>311-325</sub>-specific CD4<sup>+</sup> T cells *via* standard  
1014 ICS assays (APCs: T=2:1). Error bars indicate ±SEM of the experimental replicates.  
1015 Two independent experiments were performed with similar results, and each  
1016 independent experiment included 3 biological replicates (D, E; n=6). \**P* < 0.05; \*\**P* <  
1017 0.01; \*\*\**P* < 0.001; \*\*\*\**P* < 0.0001 and ns *P* > 0.05 (determined by one-way ANOVA  
1018 followed by a Dunnett test). NA means not available.

1019

1020 **Figure 8. Lack of *Beclin1* or *Atg7* decreases endogenous IAV antigen presentation**  
1021 **to *ex vivo* polyclonal CD4<sup>+</sup> T cells.**

1022 B6 mice were intranasally infected with 100 pfu of PR8. Primary T cells were collected  
1023 from BAL washes and spleens at 10 dpi. Endogenous IAV antigen presentation to (A)  
1024 primary CD4<sup>+</sup> T cells in BAL washes (top) and spleens (bottom) were assessed by  
1025 mock-infected or PR8-infected DC2.4-*FgH1tUTG* (control), DC2.4-*Beclin1*<sup>-/-</sup>, or  
1026 DC2.4-*Atg7*<sup>-/-</sup> cells *via* standard ICS assays (APCs:T=2:1). (B) Selected peptides  
1027 (HA<sub>13-30</sub>, HA<sub>19-36</sub>, NA<sub>25-42</sub>, NA<sub>37-54</sub>, NA<sub>43-60</sub>, NP<sub>43-60</sub>, NP<sub>49-66</sub>, and NP<sub>55-72</sub>) covering the  
1028 reported novel epitopes (NP<sub>45-61</sub>, NP<sub>47-63</sub>, NP<sub>52-68</sub>, HA<sub>16-32</sub>, NA<sub>25-39</sub>, and NA<sub>41-55</sub>) and 3  
1029 other positive control peptides (NP<sub>311-325</sub>, PB<sub>2106-120</sub>, and PA<sub>456-470</sub>) were used to assess  
1030 CD4<sup>+</sup> T cell response to IAV infection in the BAL washes and the spleens by standard  
1031 ICS assays. Cells in the BAL washes from 4 independent mice were pooled together

1032 for the analysis, while the cells in each spleen were separately assessed. *NIL* indicates  
1033 no peptide addition. Error bars in the spleen group indicate  $\pm$  SEM of 4 mice (n=4) per  
1034 group. Experiments were performed twice with similar results (n=8). \* $P < 0.05$ ; \*\* $P <$   
1035  $0.01$ ; \*\*\* $P < 0.001$ ; \*\*\*\* $P < 0.0001$  and ns  $P > 0.05$  (determined by one-way ANOVA  
1036 followed by a Dunnett test).

1037

1038 **Figure 9. Autophagosomes fuse with MIIC after IAV infection.**

1039 DC2.4 cells were infected with (A) PR8 or (B) X31 (MOI=1) or (C) mock-infected for  
1040 24 h before being stained by anti-LC3, anti-NP, anti-I-A<sup>b</sup> and anti-H2-M antibodies.  
1041 Scale bar: 10  $\mu$ m. The intensity profile of the region of interest (ROI) lines show the  
1042 consistent intensity of green and red channels respectively, which present the co-  
1043 localization between the two channels. Experiments were performed 3 times (n=3) with  
1044 similar results.

1045

1046

1047

1048

1049

1050

1051

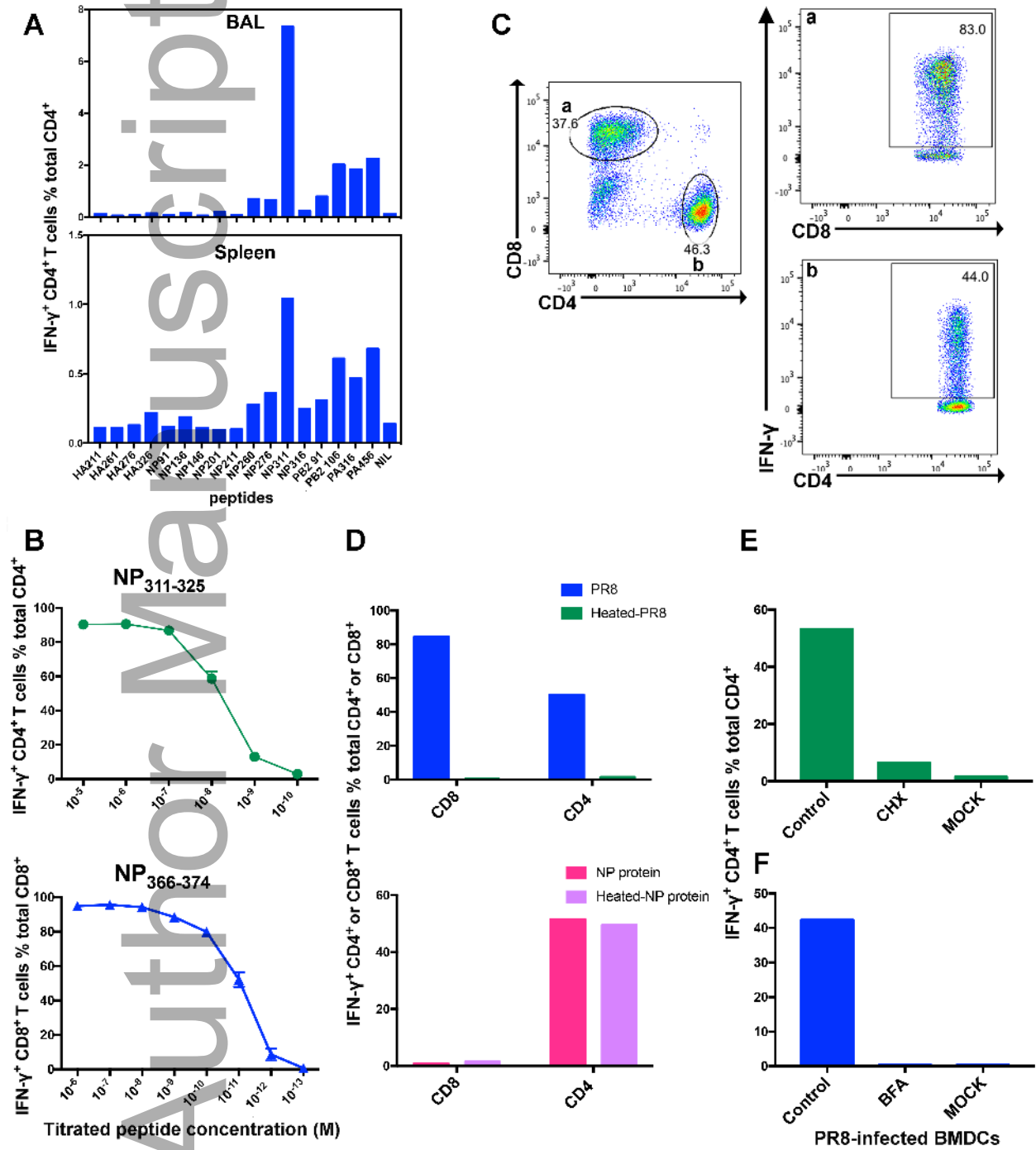
1052

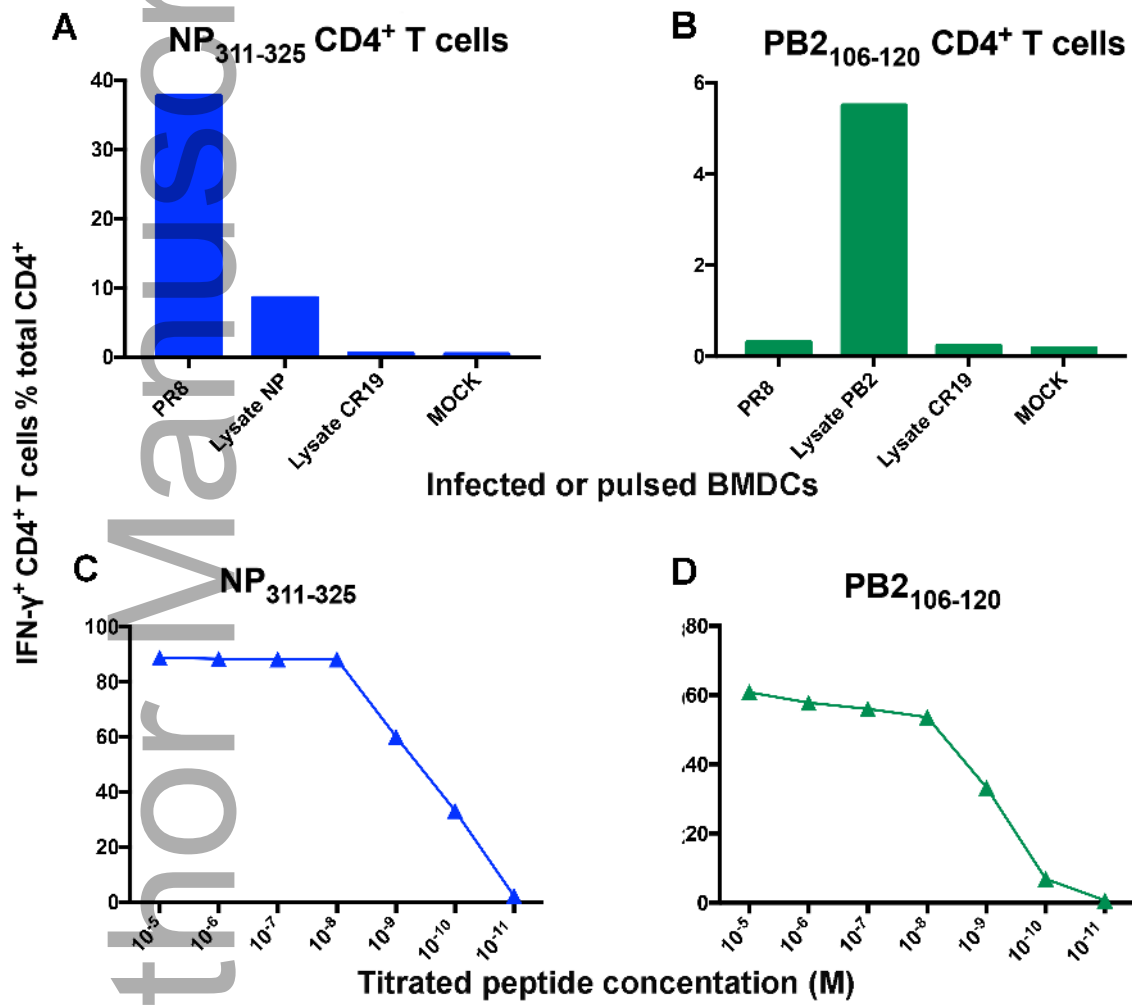
1053

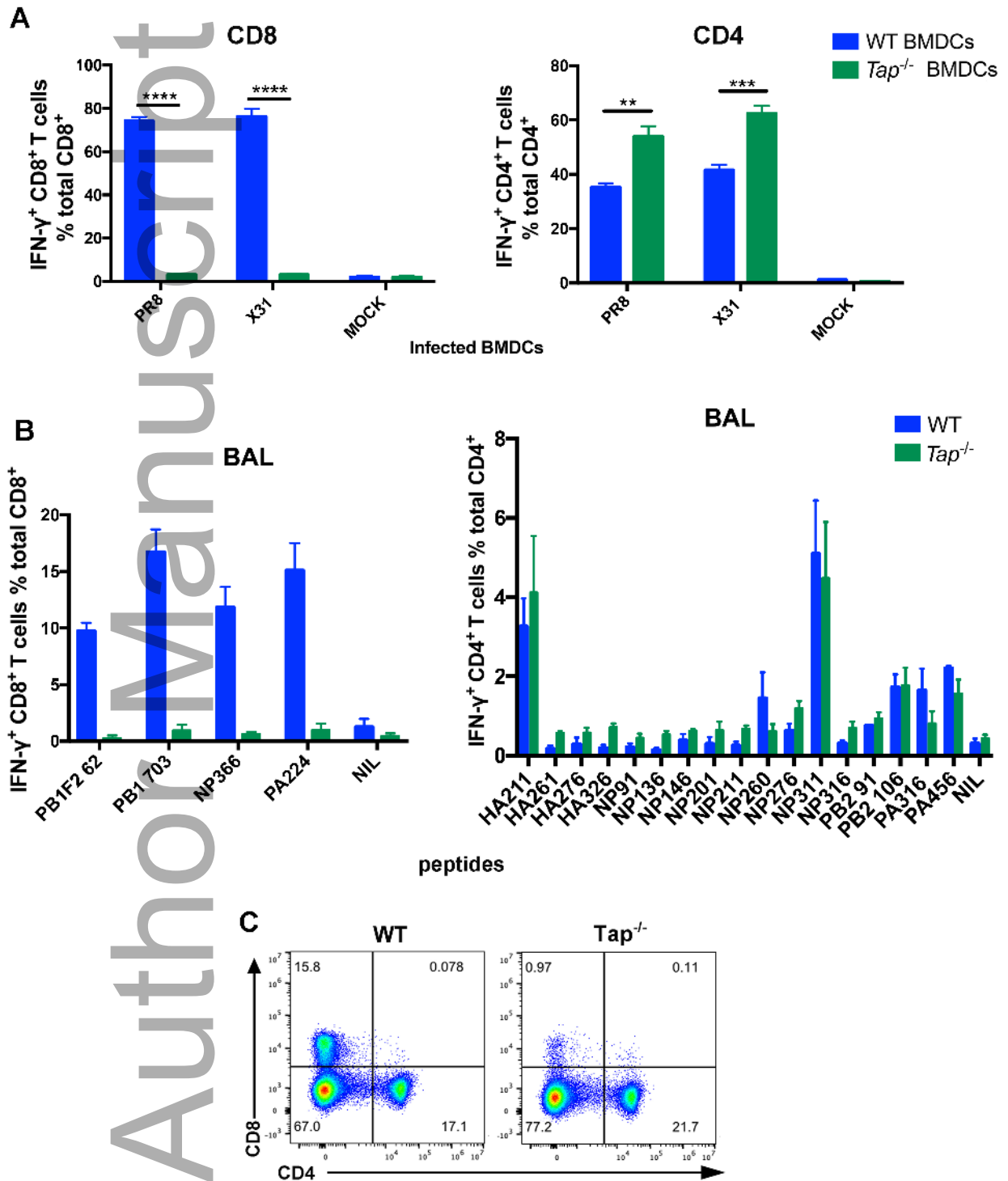
1054 **Table 1 Peptide information**

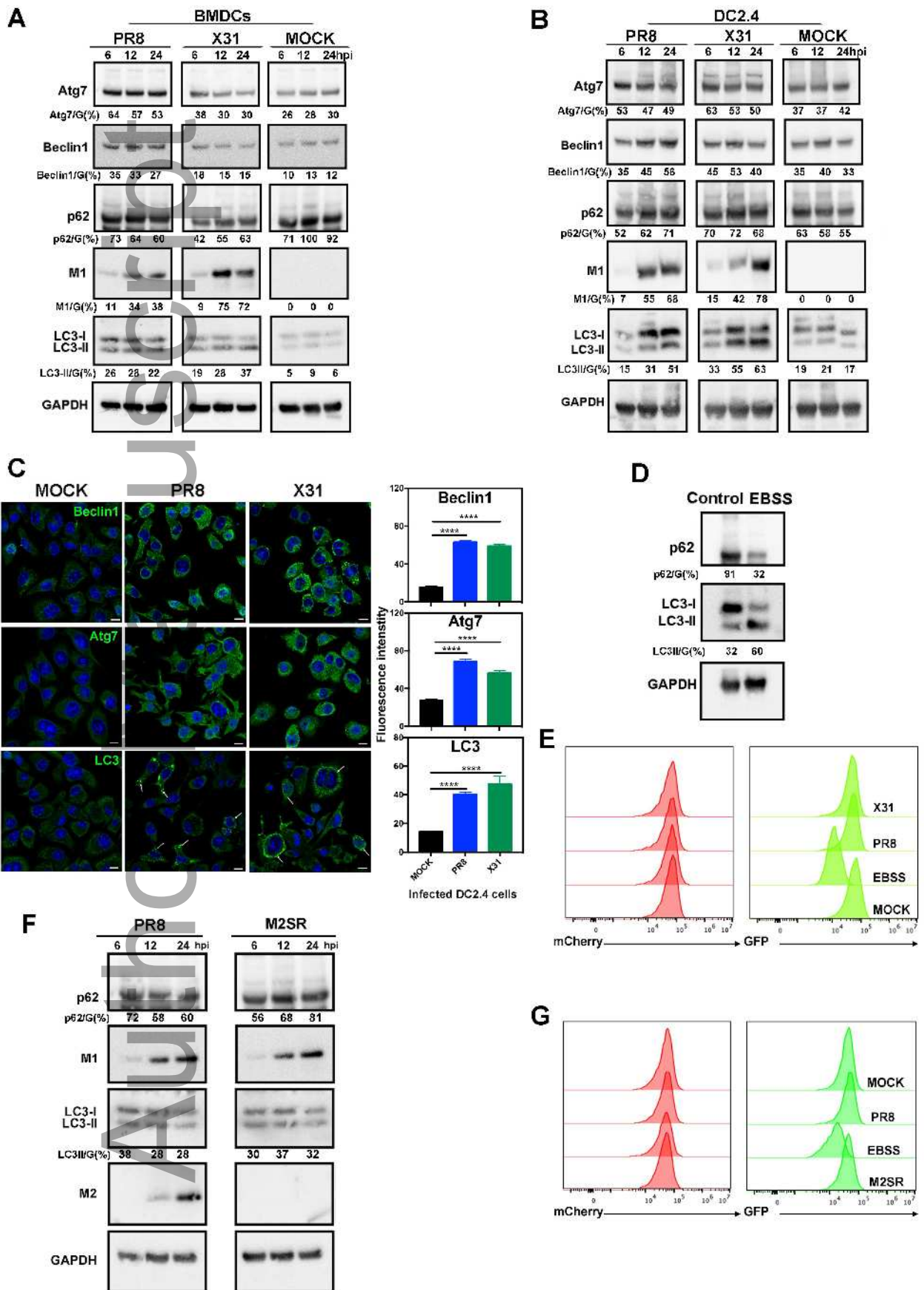
Peptide name	Sequence
HA <sub>211-225</sub>	YVQASGRVTVSTRRS
HA <sub>261-275</sub>	INSNGNLIAPRGYFK
HA <sub>276-290</sub>	MRTGKSSIMRSDAPI
HA <sub>326-340</sub>	KQNTLKLATGMRNVP

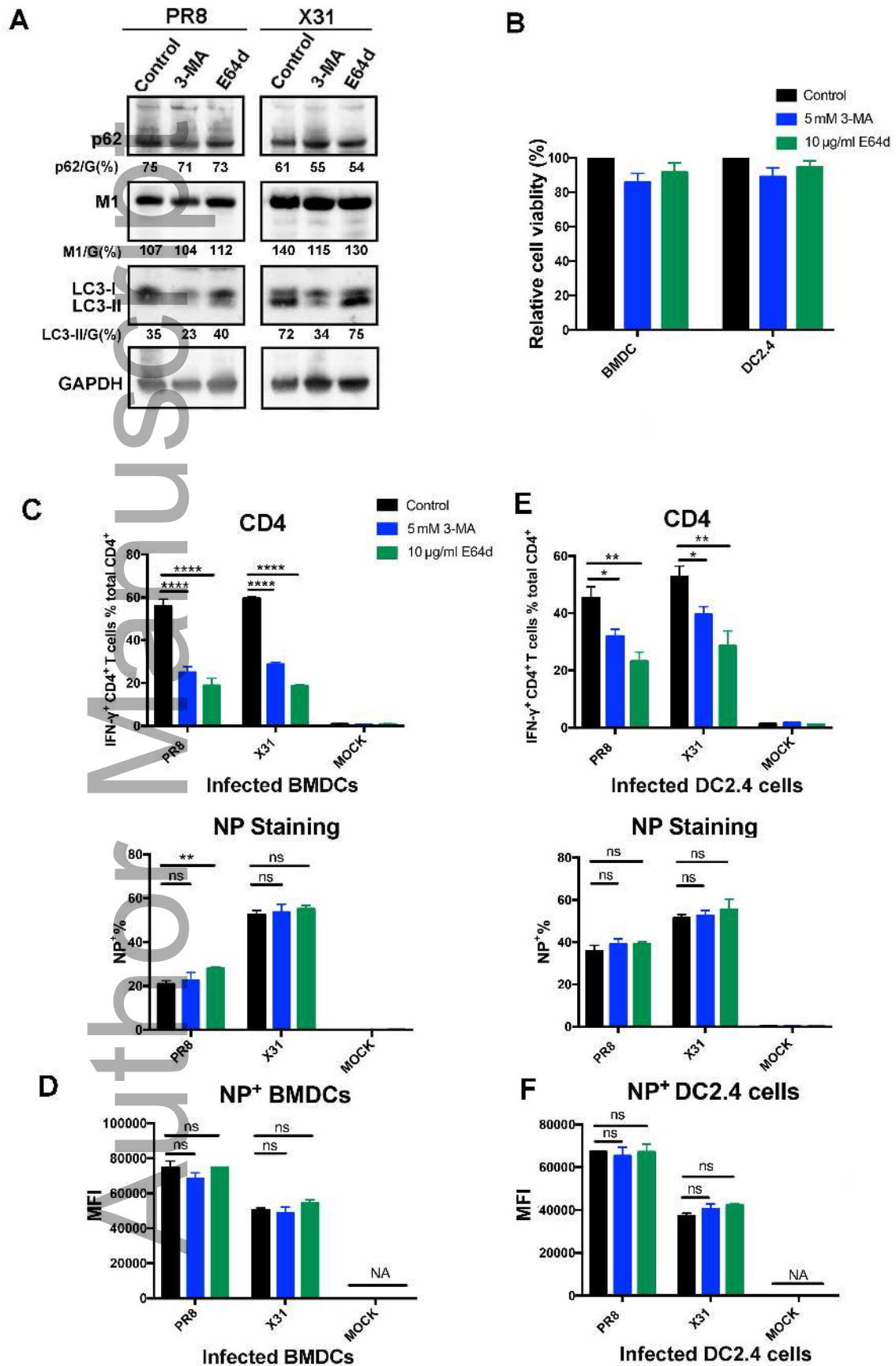
NP <sub>91-105</sub>	KTGGPIYRRVNGKWM
NP <sub>136-150</sub>	MMIWHSNLNDATYQR
NP <sub>146-160</sub>	ATYQORTRALVRTGMD
NP <sub>201-215</sub>	INDRNFWRGENGRKT
NP <sub>211-225</sub>	NGRKTRIAYERMENI
NP <sub>260-273</sub>	ARSALILRGVVAHK
NP <sub>276-290</sub>	LPACVYGPVAVASGYD
NP <sub>311-325</sub>	QVYSLIRPNENPAHK
NP <sub>316-330</sub>	IRPNENPAHKSQLVW
PB <sub>291-105</sub>	VSP LAVTWWNRNGPM
PB <sub>2106-120</sub>	TNTVHYPKIYKTYFE
PA <sub>316-330</sub>	GWKEPNVVKPHEKGI
PA <sub>456-470</sub>	RATEYIMKGVYINTA
PA <sub>224-233</sub>	SSELENFRAYV
PB1F <sub>262-70</sub>	LSLRNPILV
PB1 <sub>703-711</sub>	SSYRRPVG I
NP <sub>366-374</sub>	ASNENMETM
NP <sub>43-60</sub>	MCTELKLSDYEGRLIQNS
NP <sub>49-66</sub>	LSDYEGRLIQNSLTIERM
NP <sub>55-72</sub>	RLIQNSLTIERMVLSAFD
HA <sub>13-30</sub>	AAADADTICIGYHANNST
HA <sub>19-36</sub>	TICIGYHANNSTDTVDTV
NA <sub>25-42</sub>	QIGNIISIWISHSIQTGS
NA <sub>37-54</sub>	SIQTGSQNHTGICNQNII
NA <sub>43-60</sub>	QNHTGICNQNIIITYKNST



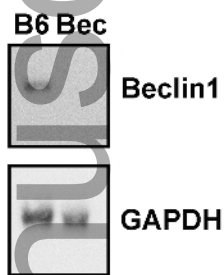




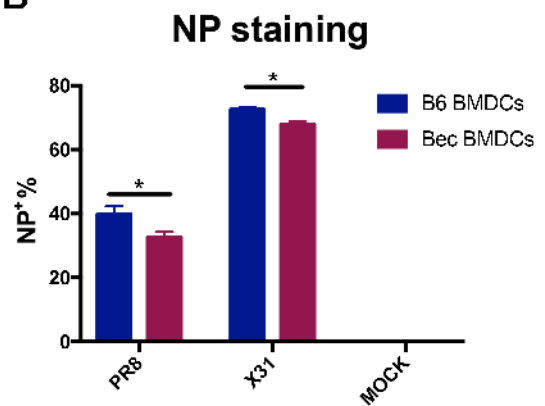




A



B



C

